On the multi-frequency obstacle reconstruction via the linear sampling method

Bojan B. Guzina[1], **Fioralba Cakoni**[2] **and Cédric Bellis**[1,3]

[1] Department of Civil Engineering, University of Minnesota, Minneapolis, MN
[2] Department of Mathematical Sciences, University of Delaware, Newark, DE
[3] Laboratoire de Mécanique des Solides, Ecole Polytechnique, Palaiseau, France

E-mail: guzina@wave.ce.umn.edu, cakoni@math.udel.edu, bellis@lms.polytechnique.fr

Abstract.
This paper investigates the possibility of multi-frequency reconstruction of sound-soft and penetrable obstacles via the linear sampling method involving either far-field or near-field observations of the scattered field. On establishing a suitable approximate solution to the linear sampling equation and making an assumption of continuous frequency sweep, two possible choices for a cumulative multi-frequency indicator function of the scatterer's support are proposed. The first alternative, termed the "serial" indicator, is taken as a natural extension of its monochromatic companion in the sense that its computation entails *space-frequency* (as opposed to space) L^2-norm of a solution to the linear sampling equation. Under a set of assumptions that include experimental observations down to zero frequency and compact frequency support of the wavelet used to illuminate the obstacle, this indicator function is further related to its time-domain counterpart. As a second possibility, the so-called "parallel" indicator is alternatively proposed as an L^2-norm, in the frequency domain, of the monochromatic indicator function. On the basis of a perturbation analysis which demonstrates that the monochromatic solution of the linear sampling equation behaves as $O(|k^2 - k_*^2|^{-m})$, $m \geqslant 1$ in the neighborhood of an isolated eigenvalue, k_*^2, of the associated interior (Dirichlet or transmission) problem, it is found that the "serial" indicator is unable to distinguish the interior from the exterior of a scatterer in situations when the prescribed frequency band traverses at least one such eigenvalue. In contrast the "parallel" indicator is, due to its particular structure, shown to be insensitive to the presence of pertinent interior eigenvalues (unknown beforehand and typically belonging to a countable set), and thus to be robust in a generic scattering configuration. A set of numerical results, including both "fine" and "coarse" frequency sampling, is included to illustrate the performance of the competing (multi-frequency) indicator functions, demonstrating behavior that is consistent with the theoretical results.

Keywords: linear sampling method, multi-frequency reconstruction, interior Dirichlet eigenvalues, transmission eigenvalues.

1. Introduction

In the context of inverse scattering, the past two decades have witnessed the inception and growth of a range of non-iterative techniques for obstacle reconstruction such as the linear sampling method [17, 16, 9, 7], the factorization method [24, 25, 27], the point source method [39], and the topological sensitivity approach [21, 4, 32]. Apart from the latter technique, these point-probing algorithms commonly operate within the framework of monochromatic i.e. single-frequency obstacle illumination which postulates that the squared wave number, computed with reference to the background medium, is not an eigenvalue of the associated interior (e.g. Dirichlet or transmission) problem. For common scattering configurations such eigenvalues form an at most countable set, with no accumulation points other than infinity [35, 40, 9, 33, 26, 13, 12], which makes the featured restriction manageable if not desirable in the context of practical applications.

Besides (and before) the choice of an appropriate reconstruction technique, the critical issue for most inverse scattering problems is the richness of the observed data set. In general the latter can be extended either spatially, in terms of the aperture of experimental observations, or temporally, by considering multi-frequency or time-domain scattered waveforms. Notwithstanding the fact that the latter alternative is often far more tractable in terms of experimental implementation, the literature dealing with point-probing algorithms that transcend the customary monochromatic framework is relatively scarce. In particular, one may mention the multi-frequency and time-domain treatments of the point source method in [30, 29, 31] as well as the time-domain formulation of the linear sampling method [14] which, by making reference to the space-time Sobolev spaces of order four, voids the need to use the Fourier transform and thus to deal with associated causality issues. What largely remains unclear, however, is the role of the eigenvalues of the germane interior problem (defined over the support of a hidden scatterer) toward the performance of point-probing methods in situations where the former are traversed by a given frequency sweep or the Fourier spectrum of a prescribed transient signal. So far, the only light in this direction was shed in [31] who demonstrated that the regularized solution density, affiliated with the point source method, is uniformly bounded with respect to the wavenumber over compact subsets of the real axis.

To help bridge the gap, this study focuses on the multi-frequency reconstruction of Dirichlet and penetrable obstacles via the linear sampling method entailing either far-field or near-field observations of the scattered field. On assuming that the (monochromatic) sampling equation is solved over a compact connected set of real-valued excitation frequencies ω, two possible choices for a cumulative, multi-frequency indicator function of the scatterer's support are considered. In the first proposition, the indicator function is taken as a reciprocal space-frequency L^2-norm of the featured solution density. Upon subtle modification this "serial" construct is shown, via the use of Plancherel identity and hypothesis that the observations of the scattered field extend toward zero frequency, to be identifiable with the corresponding time-domain indicator function. To furnish an alternative, a "parallel" indicator function is also proposed as an L^2-norm, in the frequency domain, of its monochromatic counterpart.

For a close examination of the utility of the proposed indicators in a generic multi-frequency environment, the developments are complemented by a perturbation analysis of the relevant interior problem, which demonstrates that the featured (linear sampling) solution density behaves as $O(|\omega-\omega_*|^{-m}),\ m\geqslant 1$ in the neighborhood of a characteristic frequency ω_* which corresponds to an isolated eigenvalue of the interior problem. This result in turn exposes the robustness of the "parallel" indicator, and futility of its "serial" companion in situations when the prescribed frequency sweep traverses at least one such ω_* – a finding that is highlighted by the fact that the support of an obstacle, and thus its (Dirichlet or transmission) eigenvalues, are unknown beforehand. A set of numerical results, assuming far-field scattering by Dirichlet and penetrable obstacles, is included to illustrate the analytical findings.

2. Preliminaries

Scattering by Dirichlet obstacle. Consider the time-harmonic scattering of scalar waves by a sound-soft obstacle D in an otherwise homogeneous unbounded medium $\mathbb{R}^3$, endowed with sound speed $c_{\rm o}$ (not necessarily real-valued), due to *either* set of incident fields

$$u^i=\begin{cases} e^{\mathrm{i}kx\cdot d}, & d\in\Omega \quad \text{(plane waves)},\\ \Psi(x,y,k), & y\in S_s \quad \text{(point sources)}.\end{cases} \tag{1}$$

Here $k=\omega/c_{\rm o}$ is the wavenumber; ω denotes the frequency of excitation;

$$\Psi(x,y,k)=\frac{1}{4\pi}\frac{e^{\mathrm{i}k|x-y|}}{|x-y|},\qquad x\neq y$$

is the radiating fundamental solution of the Helmholtz equation; Ω is the unit sphere centered at the origin; S_s is a suitable surface containing the point sources used to illuminate the obstacle, and $c_{\rm o}$ is such that its real and imaginary parts are respectively $\mathcal{R}(c_{\rm o})>0$ and $\mathcal{I}(c_{\rm o})\leqslant 0$. The support of D is assumed to be such that $\mathbb{R}^3\setminus\overline{D}$ is connected, and that ∂D is of Lipschitz type. With such premises the direct scattering problem can be written as

$$\begin{aligned} \Delta u+k^2u&=0 \qquad \text{in}\quad \mathbb{R}^3\setminus\overline{D},\\ u&=-u^i \qquad \text{on}\quad \partial D,\\ \lim_{|x|\to\infty}|x|\left(\frac{\partial u}{\partial|x|}-\mathrm{i}ku\right)&=0, \end{aligned} \tag{2}$$

where the Sommerfeld radiation condition holds uniformly with respect to $\hat{x}=x/|x|$. It is well known [18] that (2) permits a unique solution $u\in H^1_{\rm loc}(\mathbb{R}^3\setminus\overline{D})$, see [**?**] for Lipschitz domains, where the field equation and the boundary condition are interpreted respectively in the sense of distributions and the sense of the trace.

Scattering by penetrable obstacle. As a canonical example of the scattering by a penetrable obstacle, consider next the case where D is characterized by a spatially-varying sound speed $c(x)$ and associated index of refraction, $n(x)=(c_{\rm o}/c)^2$, such that i) $\mathcal{R}(c)>c_{\rm D}>0$ and

$\mathcal{I}(c) \leqslant 0$ where $c_{\scriptscriptstyle D}$ is a constant; ii) $n \in L_\infty(D)$, and iii) ∇n is sufficiently small so that it can be omitted from the field equation. For simplicity of exposition, an additional hypothesis is made that the mass density of the system, ρ, is constant throughout (this restriction can however be relaxed, see Remark 3). On retaining the hypotheses on the geometry of D as in the sound-soft case, the relevant scattering problem can be written as

$$\begin{aligned} \Delta u + k^2 u = 0 \qquad & \text{in} \quad \mathbb{R}^3 \setminus \overline{D}, \\ \Delta \varpi + k^2 n\, \varpi = 0 \qquad & \text{in} \quad D, \\ \varpi - u = u^i, \quad \varpi_{,\nu} - u_{,\nu} = u^i_{,\nu} \qquad & \text{on} \quad \partial D, \\ \lim_{|x|\to\infty} |x| \left(\frac{\partial u}{\partial |x|} - \mathrm{i}ku \right) = 0, & \end{aligned} \tag{3}$$

where $u_{,\nu} = \nabla u \cdot \nu$, and ν is the normal on ∂D (defined almost everywhere) oriented toward the exterior of D. Similar to the case of scattering by a Dirichlet obstacle, it is known [18, **?**] that (3) permits a unique solution $(u, \varpi) \in H^1_{\text{loc}}(\mathbb{R}^3 \setminus \overline{D}) \times H^1(D)$.

By way of Green's theorem, it can be shown [18] that the scattered field u solving either (2) or (3) permits integral representation

$$u(x, \star) = \int_{\partial D} \Big(u(\xi, \star) \Psi_{,\nu}(x, \xi, k) - u_{,\nu}(\xi, \star) \Psi(x, \xi, k) \Big) \mathrm{d}s_\xi, \quad \begin{cases} \star = d \in \Omega & \text{(plane waves)}, \\ \star = y \in S_s & \text{(point sources)} \end{cases} \tag{4}$$

which, assuming illumination by plane waves, exposes its asymptotic behavior

$$u(x, d) \;=\; \frac{e^{\mathrm{i}k|x|}}{|x|} u_\infty(\hat{x}, d) \;+\; O\left(|x|^{-2}\right) \qquad \text{as} \quad |x| \to \infty, \tag{5}$$

where

$$u_\infty(\hat{x}, d) \;=\; \int_{\partial D} \Big(u(\xi, d) (e^{-ik\hat{x}\cdot\xi})_{,\nu} \;-\; u_{,\nu}(\xi, d) e^{-ik\hat{x}\cdot\xi} \Big) \mathrm{d}s_\xi \tag{6}$$

is the so-called far-field pattern of the scattered field [18].

3. Inverse scattering via the linear sampling method

With reference to the direct scattering framework established earlier, the goal is to reconstruct the support D of a hidden obstacle on the basis of available information on the scattered field, synthesized via u_∞ or u, for multiple incident fields. Depending on the character and nature of such data, however, it is useful to distinguish between the "far-field" and "near-field" inverse scattering problems as described in the sequel. For the remainder of this section it is assumed, following the usual treatment [18, 16], that the data are available at a single excitation frequency, ω, such that k^2 is not a *Dirichlet eigenvalue* [18] for the bounded domain D when dealing with sound-soft obstacles, nor a *transmission eigenvalue* [40, 19] for D when dealing with penetrable scatterers.

Far-field observations. For this configuration, it is for simplicity assumed that the far-field pattern u_∞ is known for every direction of observation and every direction of plane-wave incidence, i.e. that the data are given by $u_\infty(\hat{x}, d)$ for $\hat{x}, d \in \Omega$ (the reader is referred to [5] for an account of the limited-aperture case). In this setting, the linear sampling method revolves around solving the equation of the first kind

$$(Fg_z)(\hat{x}) \;=\; \Psi_\infty(\hat{x}, z, k), \qquad \hat{x} \in \Omega, \tag{7}$$

where $F : L^2(\Omega) \to L^2(\Omega)$ is the so-called far-field operator given by

$$(Fg)(\hat{x}) := \int_\Omega u_\infty(\hat{x}, d)\, g(d)\, \mathrm{d}s_d; \tag{8}$$

g_z is the solution density used to construct an indicator function; z denotes the sampling point, and Ψ_∞ is the far-field pattern of Ψ, namely

$$\Psi_\infty(\hat{x}, z, k) \;=\; \tfrac{1}{4\pi} e^{-\mathrm{i}k\hat{x}\cdot z}, \qquad \Psi(x, z, k) = \frac{e^{\mathrm{i}k|x|}}{|x|}\Psi_\infty(\hat{x}, z, k) + O\left(|x|^{-2}\right) \quad \text{as} \quad |x| \to \infty. \tag{9}$$

With such premises, it can be shown [6], [27] that

- If $z \in D$ then for every $\epsilon > 0$, there exists a solution $g_z^\epsilon \in L^2(\Omega)$ of (7) such that

$$\| Fg_z^\epsilon(\cdot) - \Psi_\infty(\cdot, z, k) \|_{L^2(\Omega)} < \epsilon; \tag{10}$$

- When $z \in D$, one further has

$$\lim_{z \to \partial D} \| g_z^\epsilon \|_{L^2(\Omega)} \to \infty, \qquad \lim_{z \to \partial D} \| v_{g_z^\epsilon} \|_X \to \infty,$$

  where

$$v_g(x) := \int_\Omega e^{\mathrm{i}kx\cdot d}\, g(d)\, \mathrm{d}s_d \tag{11}$$

  is the Herglotz wave function with kernel g, and

- When $z \in \mathbb{R}^3 \setminus \overline{D}$, then for every $\epsilon > 0$ there exists a solution $g_z^\epsilon \in L^2(\Omega)$ such that

$$\| Fg_z^\epsilon(\cdot) - \Psi_\infty(\cdot, z, k) \|_{L^2(\Omega)} < \epsilon$$

  and

$$\lim_{\epsilon \to 0} \| g_z^\epsilon \|_{L^2(\Omega)} \to \infty, \qquad \lim_{\epsilon \to 0} \| v_{g_z^\epsilon} \|_X \to \infty$$

where $X := H^1(D)$ when considering (2), and $X := L^2(D)$ when considering (3).
With the above result in place, D can be reconstructed by employing a suitable regularization technique to solve the far-field equation $Fg_z = \Psi_\infty(\cdot, z, k)$ over an appropriate grid of sampling points, and using $\Pi(z) := 1/\| g_z \|_{L^2(\Omega)}$ as a characteristic function of the support of the scatterer.

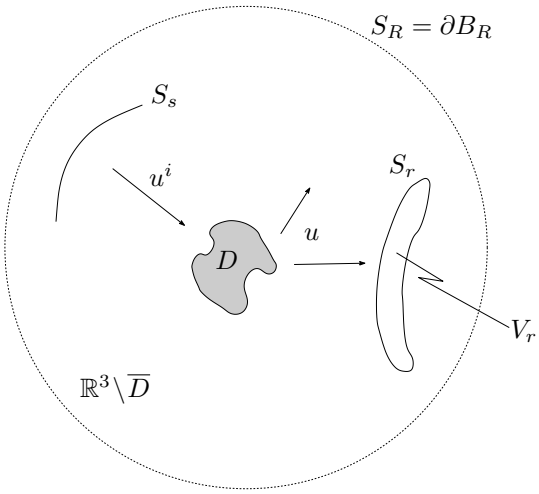

Figure 1: Near-field scattering configuration.

Near-field observations. In this case it is assumed that the obstacle is illuminated using point sources located on the source surface S_s, while the scattered field is monitored over a (union of) *closed* C^1 surface(s) S_r, see Fig. 1. Accordingly the data is given by $u(x, y)$ for $x \in S_r$ and $y \in S_s$. Hereon it is assumed that $S_s \cap D = \emptyset$ and $S_r \cap D = \emptyset$, with no restrictions imposed on the intersection between S_s and S_r. For further reference, let V_r denote the finite domain bounded by S_r whereby $\partial V_r = S_r$. Assuming further that k^2 is not a Dirichlet eigenvalue for V_r (see Remark 1), the near-field counterpart of (7), see e.g. [16], can be written as

$$(Ng_z)(x) \;=\; \Psi(x, z, k), \qquad x \in S_r, \tag{12}$$

where $N : L^2(S_s) \to L^2(S_r)$ is the so-called near-field operator given by

$$(Ng)(x) := \int_{S_s} u(x, y)\, g(y)\, \mathrm{d}s_y. \tag{13}$$

With the aforementioned restriction on k, the existence of a unique solution to the interior Dirichlet problem over V_r guarantees that, when (12) is met, sound fields $Ng_z(\cdot)$ and $\Psi(\cdot, z, k)$ share the Cauchy data on S_r. By way of Holmgren's uniqueness theorem [34], this result in turn helps ensure that the solution of the near-field equation (12) possesses approximation and unboundedness properties that mirror those of its far-field counterpart (see e.g. [22] in the context of elastodynamics), namely

- If $z \in D$ then for every $\epsilon > 0$, there exists a solution $g_z^\epsilon \in L^2(S_s)$ of (12) such that

$$\| Ng_z^\epsilon(\cdot) - \Psi(\cdot, z, k) \|_{L^2(S_r)} < \epsilon; \tag{14}$$

- When $z \in D$, one additionally has

$$\lim_{z \to \partial D} \| g_z^\epsilon \|_{L^2(S_s)} \to \infty, \qquad \lim_{z \to \partial D} \| \vartheta_{g_z^\epsilon} \|_X \to \infty,$$

  where

$$\vartheta_g(x) := \int_{S_s} \Psi(x, y, k)\, g(y)\, \mathrm{d}s_y \tag{15}$$

  is a single-layer potential with density g, and

- When $z \in \mathbb{R}^3 \setminus (\overline{D} \cup S_s \cup S_r)$, then for every $\epsilon > 0$ there exists a solution $g_z^\epsilon \in L^2(S_s)$ such that

$$\| N g_z^\epsilon(\cdot) - \Psi(\cdot, z, k) \|_{L^2(S_r)} < \epsilon$$

and

$$\lim_{\epsilon \to 0} \| g_z^\epsilon \|_{L^2(S_s)} \to \infty, \qquad \lim_{\epsilon \to 0} \| \vartheta_{g_z^\epsilon} \|_X \to \infty,$$

where $X := H^1(D)$ when considering (2), and $X := L^2(D)$ when considering (3).

Similar to the case of far-field observations, the support of D can in this case be exposed by computing a regularized solution of the near-field equation $N g_z = \Psi(\cdot, z, k)$ over an appropriate grid of sampling points, and deploying $\Pi(z) := 1/\| g_z \|_{L^2(S_s)}$ as a characteristic function of the support of the scatterer.

3.1. Relationship with the solution to the interior problem

To shed light on the denseness claims (10) and (14), let $\overline{\mathbb{H}} = \{v \in H^1(D) : \Delta v + k^2 v = 0\}$ and $\overline{\mathbb{L}} = \{v \in L^2(D) : \Delta v + k^2 v = 0\}$ denote respectively the closures of the space of $C^2(D)$ solutions to the Helmholtz equation in D with respect to the $H^1(D)$-norm and the $L^2(D)$-norm. In what follows, the sought relationship between an approximate solution to the linear sampling equation and that of the companion interior problem will be exposed for situations featuring either Dirichlet or penetrable scatterers, and testing configurations involving either far-field or near-field observations. Owing to the fact that this relationship has so far been investigated solely on a case-specific basis (see e.g. [7] and references therein), the study proceeds with a unifying treatment of the problem, starting with inverse scattering by a Dirichlet obstacle in a near-field setting. Here it is particularly important to note that the ensuing estimates, while established in a time-harmonic setting, hold *uniformly* with respect to k over any closed region in the complex plane (hereon denoted by $\mathbb{C}$) – a result that provides a linchpin for the extension of the linear sampling to multi-frequency scattering configurations.

Dirichlet obstacle. First, consider the scattering by a sound-soft obstacle (2) and associated (interior) Dirichlet problem

$$\begin{aligned} \Delta v_z + k^2 v_z &= 0 \qquad \text{in} \quad D, \\ v_z + \Psi(\cdot, z, k) &= 0 \qquad \text{on} \quad \partial D \end{aligned} \tag{16}$$

at vibration frequency ω such that k^2 is not a Dirichlet eigenvalue for D. Under the latter assumption, it is known that (16) admits a unique solution $v_z \in H^1(D)$.

As shown in [20], the set $\mathbb{F}_{\scriptscriptstyle F} = \{v_g|_D : g \in L^2(\Omega)\}$ of Herglotz wave functions (11) with square-integrable kernel g is dense in $\overline{\mathbb{H}}$ with respect to the $H^1(D)$ norm. In the context of near-field observations, the same approximation property in $\overline{\mathbb{H}}$ can be established for the set of single-layer potentials (15) with square-integrable kernel $\mathbb{F}_{\scriptscriptstyle N} = \{\vartheta_g|_D : g \in L^2(S_s)\}$. Indeed, the proof of this claim follows along the lines of Section 2.3 in [5] where, for the purpose of this study, quantity "V_g" should be superseded by single-layer potential (15).

Lemma 1. *Assume that $z \in D$, and let k be such that $|k - k_0| \leqslant r$ for some $r > 0$ and $k_0 \in \mathbb{C}$. Under such hypotheses there is a constant c_0 independent of k (but dependent on k_0 and r), such that any density $g_z^\epsilon \in L^2(S_s)$ for which the associated single-layer potential (15) approximates the unique solution of (16) as $\| \vartheta_{g_z^\epsilon} - v_z \|_{H^1(D)} < c_0\epsilon$, also satisfies the near-field inequality (14). In addition, for any $\epsilon > 0$ there exists density $g_z^\epsilon \in L^2(S_s)$ such that $\vartheta_{g_z^\epsilon}$ satisfies the prescribed $H^1(D)$ inequality.*

Proof. Let $\mathcal{B} : H^{1/2}(\partial D) \to L^2(S_r)$ denote the linear operator that maps functions $f \in H^{1/2}(\partial D)$ to $u|_{S_r}$, where $u \in H^1_{loc}(\mathbb{R}^3 \setminus \overline{D})$ is the unique radiating solution to the exterior Dirichlet problem with boundary data f, i.e. u satisfies (2) with $-u^i$ replaced by f. By virtue of the embedding of $H^{1/2}(S_r)$ in $L^2(S_r)$, the well-posedness of the exterior Dirichlet problem, Green's representation formula (4) for u, and the boundedness of the Dirichlet-to-Neumann mapping whereby $\|u_{,\nu}\|_{H^{-1/2}(\partial D)} \leqslant C\|u\|_{H^{1/2}(\partial D)}$ for some $C > 0$, one finds that

$$\|\mathcal{B}f\|_{L^2(S_r)} = \|u\|_{L^2(S_r)} \leqslant \|u\|_{H^{1/2}(S_r)} \leqslant c_1\|f\|_{H^{1/2}(\partial D)} \tag{17}$$

for some $c_1 > 0$. Owing to the fact that the solution to the exterior Dirichlet problem depends continuously on k, constant c_1 can be further chosen independent of k such that (17) holds everywhere within the ball $|k - k_0| \leqslant r$, whereby $\mathcal{B}$ is *uniformly* bounded from $H^{1/2}(\partial D)$ to $L^2(S_r)$ with respect to k in $|k - k_0| \leqslant r$. Since $(\Delta + k^2)\Psi(\cdot, z, k) = 0$ in $\mathbb{R}^3 \setminus \overline{D}$ for $z \in D$, one obviously has $\mathcal{B}\Psi(\cdot, z, k) = \Psi(\cdot, z, k)|_{S_r}$. With reference to (13), on the other hand, it follows by the linearity of the problem that the near-field operator can be decomposed as $N = \mathcal{B}\mathcal{P}$, where $\mathcal{P}g := -\vartheta_g|_{\partial D}$. Next, let $g_z^\epsilon \in L^2(S_s)$ be such that $\| \vartheta_{g_z^\epsilon} - v_z \|_{H^1(D)} < c_0\epsilon$. By virtue of the trace theorem and the fact that v_z solves (16), one has

$$\|\mathcal{P}g_z^\epsilon - \Psi(\cdot, z, k)\|_{H^{1/2}(\partial D)} \leqslant c_2\|\vartheta_{g_z^\epsilon} - v_z\|_{H^1(D)},$$

where c_2 is independent of k. Thus

$$\begin{aligned} \| Ng_z^\epsilon(\cdot) - \Psi(\cdot, z, k) \|_{L^2(S_r)} &= \|\mathcal{B}\mathcal{P}g_z^\epsilon - \mathcal{B}\Psi(\cdot, z, k)\|_{L^2(S_r)} \\ &= \|\mathcal{B}(\mathcal{P}g_z^\epsilon - \Psi(\cdot, z, k))\|_{L^2(S_r)} \leqslant c_1\|\mathcal{P}g_z^\epsilon - \Psi(\cdot, z, k)\|_{H^{1/2}(\partial D)} \leqslant c_1c_2c_0\,\epsilon \end{aligned} \tag{18}$$

and, by taking $0 < c_0 < (c_1c_2)^{-1}$,

$$\| Ng_z^\epsilon(\cdot) - \Psi(\cdot, z, k) \|_{L^2(S_r)} < \epsilon.$$

By the denseness property of $\mathbb{F}_N$ in $\overline{\mathbb{H}}$ stipulated earlier, for any $c_0\epsilon > 0$ and $v_z \in \overline{\mathbb{H}}$ there is a single-layer potential (15) with density $g_z^\epsilon \in L^2(S_s)$ such that

$$\| \vartheta_{g_z^\epsilon} - v_z \|_{H^1(D)} < c_0\epsilon,$$

which establishes the claim of the lemma. □

Lemma 2. *Let $z \in D$, and let k be such that $|k - k_0| \leqslant r$ for some $r > 0$ and $k_0 \in \mathbb{C}$. With such premises there exists constant c_0 independent of k (but dependent on k_0 and r), such that any density $g_z^\epsilon \in L^2(\Omega)$ for which the affiliated Herglotz wave function (11) approximates the*

unique solution of (16) as $\| v_{g_z^\epsilon} - v_z \|_{H^1(D)} < c_0\epsilon$*, also satisfies the far-field inequality (10). Further, for any* $c_0\epsilon > 0$ *there is density* $g_z^\epsilon \in L^2(\Omega)$ *such that* $v_{g_z^\epsilon}$ *satisfies the postulated* $H^1(D)$ *inequality.*

Proof. Here the proof mirrors that of Lemma 1, provided that i) $\mathcal{B}: H^{1/2}(\partial D) \to L^2(\Omega)$ maps any $f \in H^{1/2}(\partial D)$ to the far-field pattern (u_∞) of the radiating solution u to the exterior Dirichlet problem with boundary data f, ii) the near-field operator N is superseded by its far-field counterpart $F: L^2(\Omega) \to L^2(\Omega)$, and iii) linear operator $\mathcal{P}g := -\vartheta_g|_{\partial D}$ is replaced by $\mathcal{H}g := -v_g|_{\partial D}$ where v_g is given by (11).

□

Penetrable obstacle. In the case of scattering by a penetrable obstacle, the relevant interior problem is the so-called *interior transmission problem* [19]

$$\begin{aligned} \Delta v_z + k^2 v_z &= 0 && \text{in} \quad D, \\ \Delta w_z + k^2 n\, w_z &= 0 && \text{in} \quad D, \\ w_z - v_z &= \Psi(\cdot, z, k) && \text{on} \quad \partial D, \\ (w_z)_{,\nu} - (v_z)_{,\nu} &= \Psi_{,\nu}(\cdot, z, k) && \text{on} \quad \partial D \end{aligned} \tag{19}$$

which is, following earlier hypothesis, considered under the restriction that k^2 is not a transmission eigenvalue for D [12] – defined as the value of k^2 for which the homogeneous counterpart of (19) permits non-trivial solution. Under such limitation, (19) permits a unique solution (v_z, w_z) understood in the sense of distributions, such that $v_z \in L^2(D)$, $w_z \in L^2(D)$, and $w_z - v_z \in H^2(D)$, see [40].

Owing to the $L^2(D)$-regularity of the solution to (19), it is next useful to make an appeal to the denseness of the set of Herglotz wave functions (11) with square-integrable kernel, namely $\mathbb{F}_{_F} = \{v_g|_D : g \in L^2(\Omega)\}$, in $\overline{\mathbb{L}}$ with respect to the $L^2(D)$ norm [18]. In the context of near-field observations, the same approximation property in $\overline{\mathbb{L}}$ holds true for the set $\mathbb{F}_{_N} = \{\vartheta_g|_D : g \in L^2(S_s)\}$ of single-layer potentials (15) with square-integrable kernel.

To facilitate the ensuing discussion, one may recall that $(\Delta + k^2)\Psi(\cdot, z, k) = 0$ in $\mathbb{R}^3 \backslash \overline{D}$ for $z \in D$ which, assuming that (v_z, w_z) solves (19), demonstrates that the "difference" field defined as $u_z := w_z - v_z$ in D and $u_z := \Psi(\cdot, z, k)$ in $\mathbb{R}^3 \backslash \overline{D}$ solves the source problem

$$\begin{aligned} &\Delta u_z + k^2 n\, u_z = k^2(1-n)v_z \qquad \text{in} \quad \mathbb{R}^3, \\ &\lim_{|x|\to\infty} |x| \left(\frac{\partial u_z}{\partial |x|} - \mathrm{i}k u_z \right) = 0 \end{aligned} \tag{20}$$

assuming the continuity of u_z and $(u_z)_{,\nu}$ across ∂D (note that $n = 1$ outside D). By writing (20) in the form of a Lippmann-Schwinger equation and slightly modifying the argument in [18], p. 215, to accommodate for the $L^\infty(D)$ index of refraction $n(x)$, one easily sees that the unique solution u_z of (20) satisfies the a priori estimate $\|u_z\|_{H^2(B_R)} \leqslant c\|v_z\|_{L^2(D)}$, where B_R is a ball of radius R containing D.

Lemma 3. *Assume that $z \in D$, and let k be such that $|k - k_0| \leqslant r$ for some $r > 0$ and $k_0 \in \mathbb{C}$. Under such restrictions there is a constant c_0 independent of k (but dependent on k_0 and r), such that any density $g_z^\epsilon \in L^2(\Omega)$ for which the affiliated Herglotz wave function (11) approximates component v_z of the unique solution (v_z, w_z) to (19) as $\| v_{g_z^\epsilon} - v_z \|_{L^2(D)} < c_0\epsilon$, also satisfies the far-field inequality (10). Further, for any $c_0\epsilon > 0$ there exists density $g_z^\epsilon \in L^2(\Omega)$ such that $v_{g_z^\epsilon}$ meets the postulated $L^2(D)$ inequality.*

Proof. Consider the space of solutions to the Helmholtz equation $\overline{\mathbb{L}} = \{v \in L^2(D) : \Delta v + k^2 v = 0\}$ equipped with the $L^2(D)$ norm, and define the linear operator $\mathcal{B} \colon \overline{\mathbb{L}} \to L^2(\Omega)$ which maps $v_z \in \overline{\mathbb{L}}$ to the far-field pattern of the radiating field u_z solving (20). From the well-posedness of the source problem (20), one concludes that $\mathcal{B}$ is uniformly bounded with respect to k in $|k - k_0| \leqslant r$, i.e. that there exists constant c_1 independent of k such that $\|\mathcal{B}v_z\|_{L^2(\Omega)} \leqslant c_1 \|v_z\|_{L^2(D)}$. By the linearity of the problem it further follows that $\mathcal{B}v_g = Fg$, where F is the far-field operator given by (8) and v_g is the Herglotz wave function with kernel g. On the basis of this result, (7) and (20), it can be shown that $\mathcal{B}v_z = \Psi_\infty(\cdot, z, k)$ whenever v_z is such that the pair (v_z, w_z) uniquely solves (19). Now let $g_z^\epsilon \in L^2(\Omega)$ for which the affiliated Herglotz wave function (11) satisfies $\| v_{g_z^\epsilon} - v_z \|_{L^2(D)} < c_0\epsilon$. As a result, one finds by taking $0 < c_0 < 1/c_1$ (independent of k in $|k - k_0| \leqslant r$) that

$$\|Fg_z^\epsilon - \Psi_\infty(\cdot, z, k)\|_{L^2(\Omega)} \;=\; \|\mathcal{B}(v_{g_z^\epsilon} - v_z)\|_{L^2(\Omega)} \;\leqslant\; c_1 \|v_{g_z^\epsilon} - v_z\|_{L^2(D)} \;\leqslant\; c_1 c_0\, \epsilon \;<\; \epsilon. \quad (21)$$

With this result in place, the claim of the lemma is established by recalling the denseness in $\overline{\mathbb{L}}$ of the set of Herglotz wave functions (11) with density $g_z^\epsilon \in L^2(\Omega)$. □

Lemma 4. *Let $z \in D$, and let k be such that $|k - k_0| \leqslant r$ for some $r > 0$ and $k_0 \in \mathbb{C}$. With such hypotheses there exists constant c_0 independent of k (but dependent on k_0 and r), such that any density $g_z^\epsilon \in L^2(S_s)$ for which the affiliated single-layer potential (15) approximates component v_z of the unique solution (v_z, w_z) to (19) as $\| \vartheta_{g_z^\epsilon} - v_z \|_{L^2(D)} < c_0\epsilon$, also satisfies the near-field inequality (14). Further, for any $c_0\epsilon > 0$ there exists density $g_z^\epsilon \in L^2(S_s)$ such that $\vartheta_{g_z^\epsilon}$ meets the featured $L^2(D)$ inequality.*

Proof. Let $\mathcal{B} \colon \overline{\mathbb{L}} \to L^2(S_r)$ denote the linear operator which maps $v_z \in \overline{\mathbb{L}}$ to $u_z|_{S_r}$, where u_z solves (20). By virtue of the trace theorem and the well-posedness of (20), it is easy to see that

$$\|\mathcal{B}v_z\|_{L^2(S_r)} \;\leqslant\; c_1 \|u_z\|_{H^{3/2}(S_r)} \;\leqslant\; c_1 c_2 \|u_z\|_{H^2(B_R)} \;\leqslant\; c_1 c_2 c_3 \|v_z\|_{L^2(D)}$$

where c_1, c_2 and c_3 can be chosen to be independent of k in $|k - k_0| \leqslant r$ due to the fact that the solution of (20) depends continuously on k. The rest of the proof follows that accompanying Lemma 3, and is omitted for brevity.

□

3.2. Regularized solution

It is well known that both the far-field equation (7) and its near-field companion (12) are ill-posed, a feature that is attributed to the compactness of the respective linear operators

$F: L^2(\Omega) \to L^2(\Omega)$ and $N: L^2(S_s) \to L^2(S_r)$. Moreover, these linear sampling equations generally do not have a solution for any sampling point z. As a result, the characteristic function of the support of a scatterer is constructed on the basis of the behavior of the Herglotz wave function (11) or single-layer potential (15), affiliated with a suitable approximate solution to these equations. In realistic situations, the kernel of F or N is further polluted by noise in the measurements which necessitates the use of regularization techniques. In the context of the linear sampling method, the key question associated with the use of any regularization scheme (e.g. Tikhonov regularization), is whether such computed solution exhibits the desired properties that make the affiliated Herglotz wave function (11) or single-layer potential (15) useful toward constructing a characteristic function of the support of a scatterer. This question was affirmatively answered in [1, 2] for the situations involving far-field scattering by both Dirichlet and penetrable obstacles. To date, however, the question remains open in the context of near-field scattering.

To affix specificity to the discussion, consider next the far-field equation (7) corresponding to either direct scattering problem (2) or (3). Denoting by F^δ the far-field operator corresponding to noise-polluted measurements of the scattered field where $\delta > 0$ is a measure of the noise level, one seeks a Tikhonov-regularized solution $g^\epsilon_{z,\delta}$ of (7), defined as a unique minimizer of the Tikhonov functional

$$\|F^\delta g^\epsilon_{z,\delta} - \Psi_\infty(\cdot, z, k)\|^2_{L^2(S^2)} \; + \; \epsilon \, \|g^\epsilon_{z,\delta}\|^2_{L^2(S^2)}, \tag{22}$$

where $\epsilon > 0$ is known as the Tikhonov regularization parameter [18]. In the context of (22), it is important to know whether such regularized solution adheres to the claim of Lemma 2 or Lemma 3, depending on the nature of the scatterer. To this end, let $\epsilon(\delta)$ be a sequence of regularization parameters such that $\epsilon(\delta) \to 0$ as $\delta \to 0$, and let $g^\epsilon_{z,\delta}$ be the minimizer of (22) with $\epsilon = \epsilon(\delta)$. In [1], it was shown assuming scattering by sound-soft obstacle (2) at wavenumber k such that k^2 is not a Dirichlet eigenvalue for D, that $v_{g^\epsilon_{z,\delta}}$, $z \in D$ converges in the $H^1(D)$-norm to the unique solution v_z of (16) as $\delta \to 0$. This argument can be carried over, verbatim, to obstacle reconstruction involving scattering by penetrable obstacles (3) provided that $n(x)$ and k are both real-valued. If the latter condition is met and k^2 is not a transmission eigenvalue for D, then $v_{g^\epsilon_{z,\delta}}$, $z \in D$ converges in the $L^2(D)$-norm to v_z as $\delta \to 0$, where v_z is such that pair (v_z, w_z) uniquely solves (19).

In concluding this section it is noted that, even though no commensurate analysis is available for a Tikhonov-regularized solution to the near-field equation (12), all numerical experiments indicate that such computed solution, $g^\epsilon_{z,\delta}$, exhibits the same properties as the "mother" approximate solution g^ϵ_z examined in Lemma 1 and Lemma 4.

4. Multi-frequency reconstruction

As examined earlier, the linear sampling method considers inverse scattering at a single excitation frequency, ω, such that $k^2 = \omega^2/c_o^2$ is not an eigenvalue of the germane interior (Dirichlet or transmission) problem for D. In the case of near-field observations, an additional restriction is made that k^2 is not a Dirichlet eigenvalue of region V_r bounded by the closed

observation surface(s) S_r; however, this restriction can be removed through a suitable adjustment of the experimental setup, see Remark 1. Assuming that ∂D is of Lipschitz type, it can be shown [35, 40, 9, 33, 26, 13, 12] that the eigenspectrum of either Dirichlet or interior transmission problem over D is at most countable with no finite accumulation points. In particular, the results show that

- The Dirichlet eigenvalues form a countable set located on the positive real axis, $\Lambda \subset \mathbb{R}^+$ with $+\infty$ as the only accumulation point. From this fact and relationship $k^2 = \omega^2/c_o^2$, it further follows that if the background medium is sound-absorbing, i.e. $\mathcal{I}(c_o) < 0$, there are no (real-valued) excitation frequencies ω that give rise to the Dirichlet eigenvalues.
- The investigation of transmission eigenvalues is at present incomplete. To date, it is known that the transmission eigenvalues $k^2 > 0$ form a real-valued, countable set with $+\infty$ as the only accumulation point, provided that both $\mathcal{I}(c_o) = 0$ and $\mathcal{I}(c) = 0$ and either $c_o < c(x)$ or $c_o > c(x)$ almost everywhere in D [12]. The set of transmission eigenvalues degenerates to an empty set, $\Lambda = \emptyset$, when *either* the background medium or the obstacle are dissipative, i.e. when either $\mathcal{I}(c_o) < 0$ and $\mathcal{I}(c) = 0$, or $\mathcal{I}(c_o) = 0$ and $\mathcal{I}(c) < 0$. If both $\mathcal{I}(c_o) < 0$ and $\mathcal{I}(c) < 0$, however, particular examples indicate the existence of (real-valued) excitation frequencies ω that give rise to (complex) transmission eigenvalues k^2 [3, 8].

Remark 1. The Dirichlet eigenvalues corresponding to region V_r, bounded by the closed observation surface(s) S_r in the case of near-field observations, can be considered as being artificially injected into the problem. At a given testing frequency, these eigenvalues are not necessarily detrimental to the linear sampling method since it is possible to adjust S_r, and thus V_r, such that the prescribed frequency of excitation does not correspond to an eigenvalue for V_r. In the context of multi-frequency obstacle reconstruction that is of interest in this study, there are two possible ways to avoid these extraneous eigenvalues. In the first approach which assumes band-limited illumination in the frequency domain, one finds by virtue of the Faber-Krahn inequality for the first Dirichlet eigenvalue of V_r (the latter is greater than $\pi k_{01}^2/|V_r|$, where k_{01} is the first zero of the spherical Bessel function j_0), that it is possible to reduce V_r so that none of its (Dirichlet) eigenvalues are triggered by the frequencies from the prescribed bandwitdh. Alternatively, one may modify the near-field testing configuration by considering an array of receivers located on an *open* surface S_r, taken as a part of an analytic surface Σ enclosing both D and S_c. On invoking the regularity of a solution to the homogeneous Helmholtz equation and the principle of analytic continuation, one finds that if the radiating fields Ng given by (13) and $\Psi(\cdot, z, k)$ coincide on S_r, they will also coincide on a closed surface $\Sigma \supset S_r$. By making an appeal to the uniqueness of the exterior Dirichlet problem outside Σ and the analytic continuation principle, one finally concludes that $Ng = \Psi(\cdot, z, k)$ wherever both are defined, which in turn implies all the results established in Section 3.

In light of Remark 1, the eigenvalues of V_r will hereon be ignored, whereby Λ should be understood as a countable set containing the relevant eigenvalues of D.

To examine the possibility and effectiveness of multi-frequency obstacle reconstruction, the ensuing study focuses on a generic situation where the scattered field due to multiple

incident wavefields, synthesized via u_∞ or u, is monitored over a *frequency band*, $\omega \in \digamma_\omega := [\omega_1, \omega_2] \subset \mathbb{R}^+,\ \omega_2 < \infty$. For clarity of exposition, all frequency-dependent quantities referred to in the sequel will have ω added to their list of arguments whereby $u(x,y)$ is superseded by $u(x,y,\omega)$, $g_z(y)$ by $g_z(y,\omega)$, and so on. In this setting, the multi-frequency counterparts of (7) and (12) can be postulated as

$$\begin{aligned} (Fg_z)(\hat{x},\omega) &= \Psi_\infty(\hat{x},z,\omega/c_\mathrm{o}), \qquad \hat{x}\in\Omega, \qquad \omega\in\digamma_\omega \\ (Ng_z)(x,\omega) &= \Psi(x,z,\omega/c_\mathrm{o}), \qquad x\in S_r, \qquad \omega\in\digamma_\omega \end{aligned} \tag{23}$$

where $F : L^2(\Omega)\times L^2(\digamma_\omega) \to L^2(\Omega)\times L^2(\digamma_\omega)$ and $N : L^2(S_s)\times L^2(\digamma_\omega) \to L^2(S_r)\times L^2(\digamma_\omega)$ are bounded linear operators such that

$$\begin{aligned} (Fg)(\hat{x},\omega) &:= \int_\Omega u_\infty(\hat{x},d,\omega)\, g(d,\omega)\, \mathrm{d}s_d, \\ (Ng)(x,\omega) &:= \int_{S_s} u(x,y,\omega)\, g(y,\omega)\, \mathrm{d}s_y. \end{aligned} \tag{24}$$

For a systematic treatment of such extended inverse scattering problem, the key issues to be addressed pertain to: i) the choice of a "cumulative" indicator function that reflects the extended data set, and ii) the situation where the chosen frequency band traverses at least one interior eigenvalue, i.e. when

$$\Lambda \cap \digamma_{k^2} \neq \emptyset, \qquad \digamma_{k^2} := \big\{k^2 : k = c_\mathrm{o}^{-1}\big(\omega_1 + \eta(\omega_2-\omega_1)\big),\ \eta\in[0,1]\big\}.$$

4.1. "Serial" indicator function

Perhaps the most obvious extension of the monochromatic indicator function, $\Pi(z) = 1/\,\|\, g_z \,\|_{L^2(\bullet)}$, can be written as

$$\Pi^{(1)}_{\digamma}(z) := \frac{1}{\|\, g_z \,\|_{L^2(\bullet)\times L^2(\digamma_\omega)}} = \left(\int_{\omega_1}^{\omega_2} ||g_z(\cdot,\omega)||^2_{L^2(\bullet)}\, \mathrm{d}\omega\right)^{-1/2}, \quad \begin{cases} \bullet = \Omega & \text{(plane waves)}, \\ \bullet = S_s & \text{(point sources)}. \end{cases} \tag{25}$$

Assuming that $\Lambda \cap \digamma_{k^2} = \emptyset$, one finds on the basis of the results highlighted in Section 3 that distribution (25), similar to its monochromatic companion, becomes vanishingly small for $z \in \mathbb{R}^3 \setminus D$ which justifies its candidacy for a characteristic function of the support of the scatterer.

Relevance to inverse scattering in the time domain. An intriguing feature of (25) resides in its appeal, upon subtle modification, to the time-domain treatment of inverse scattering via linear sampling – a proposition that is currently in its early stages [14]. To investigate this possibility, it is instructive to consider an auxiliary frequency function $\mathcal{W}\in C^1(\mathbb{R})$, compactly supported over interval $[-\omega_2,\omega_2]$, and to modify (25) by setting $\omega_1 = 0$ and weighting the integrand on the right-hand side by $2|\mathcal{W}|$. Such modified indicator function can be written as

$$\Pi^{(1)}_{\digamma,\mathcal{W}}(z) = \left(\int_0^{\omega_2} 2|\mathcal{W}(\omega)|\ ||g_z(\cdot,\omega)||^2_{L^2(\bullet)}\, \mathrm{d}\omega\right)^{-1/2}. \tag{26}$$

To maintain physical relevance, it is further assumed that $\mathcal{W}(-\omega) = \overline{\mathcal{W}}(\omega)$, where overbar signifies complex conjugation. As a result, the restriction of $2|\mathcal{W}|$ to $\digamma_\omega = [0, \omega_2]$ can be interpreted as the one-sided, compactly-supported Fourier amplitude spectrum of a given wavelet, e.g. the raised cosine function [36].

Here it is useful to note that the scattered field $u(x, y, \omega)$ and fundamental solution $\Psi(x, z, \omega/c_\mathrm{o})$, together with their far-field patterns $u_\infty(\hat{x}, d, \omega)$ and $\Psi_\infty(\hat{x}, z, \omega/c_\mathrm{o})$ in (23) and (24) permit physical interpretation as the Fourier transforms of their respective time-domain companions, $\tilde{u}(x, y, t)$, $\tilde{\Psi}(x, z, t)$, $\tilde{u}_\infty(\hat{x}, d, t)$ and $\tilde{\Psi}_\infty(\hat{x}, z, t)$. Owing to the fact that the latter four quantities, which all signify relevant solutions to the wave equation, are necessarily real-valued, it follows that

$$\begin{aligned} h(\cdot, \cdot, -\omega) &= \overline{h}(\cdot, \cdot, \omega), & h &\in \{u_\infty, u\}, \\ \Phi(\cdot, \cdot, -\omega/c_\mathrm{o}) &= \overline{\Phi}(\cdot, \cdot, \omega/c_\mathrm{o}), & \Phi &\in \{\Psi_\infty, \Psi\}. \end{aligned} \tag{27}$$

On the basis of (27), the consideration and solution of (23) can, for a given data set (u_∞ or u) specified over $\digamma_\omega = [0, \omega_2]$, be formally extended to the frequency range $[-\omega_2, \omega_2]$ such that $g_z(\cdot, -\omega) = \overline{g}_z(\cdot, \omega)$.

In this setting, either of (23) can be conveniently modified by extending its frequency support to $[-\omega_2, \omega_2]$, and weighting its right-hand side by $\mathcal{W}$, namely

$$\begin{aligned} (F g_z^{\mathcal{W}})(\hat{x}, \omega) &= \mathcal{W}(\omega)\, \Psi_\infty(\hat{x}, z, \omega/c_\mathrm{o}), & \hat{x} &\in \Omega, & \omega &\in [-\omega_2, \omega_2], \\ (N g_z^{\mathcal{W}})(x, \omega) &= \mathcal{W}(\omega)\, \Psi(x, z, \omega/c_\mathrm{o}), & x &\in S_r, & \omega &\in [-\omega_2, \omega_2]. \end{aligned} \tag{28}$$

In situations where $\Lambda \cap \mathbb{R} = \emptyset$ i.e. when there are no interior eigenvalues on the real axis, the modified indicator function (26) accordingly carries the physical meaning of

$$\Pi^{(1)}_{F,\mathcal{W}}(z) = \frac{1}{2 \,\| g_z^{\mathcal{W}} \|_{L^2(\bullet) \times L^2(\digamma_\omega)}} = \frac{1}{\| g_z^{\mathcal{W}} \|_{L^2(\bullet) \times L^2([-\omega_2, \omega_2])}} = \frac{1}{\| g_z^{\mathcal{W}} \|_{L^2(\bullet) \times L^2(\mathbb{R})}}, \tag{29}$$

owing to the compact support of $\mathcal{W}$ and injectivity of F and N [16, 9].

With the above results in place, one may take the inverse Fourier transform of (28) with respect to ω to formally arrive at a *time-domain* variant of the linear sampling method, namely

$$\begin{aligned} (\tilde{F} \tilde{g}_z^{\mathcal{W}})(\hat{x}, t) &= \tilde{\Psi}_\infty^{\mathcal{W}}(\hat{x}, z, t), & \hat{x} &\in \Omega, & t &\in \mathbb{R}, \\ (\tilde{N} \tilde{g}_z^{\mathcal{W}})(x, t) &= \tilde{\Psi}^{\mathcal{W}}(x, z, t), & x &\in S_r, & t &\in \mathbb{R}. \end{aligned} \tag{30}$$

Here $\tilde{g}_z^{\mathcal{W}}$ denotes the inverse Fourier transform of $g_z^{\mathcal{W}}$; $\tilde{\Psi}^{\mathcal{W}}(\cdot, z, t)$ and $\tilde{\Psi}_\infty^{\mathcal{W}}(\cdot, z, t)$ are respectively the radiating Green's function for the wave equation in $\mathbb{R}^3$ due to "wavelet" point source $\delta(x - z)\tilde{\mathcal{W}}(t)$ and its far-field pattern, while $\tilde{F} : L^2(\Omega) \times L^2(\mathbb{R}) \to L^2(\Omega) \times L^2(\mathbb{R})$ and $\tilde{N} : L^2(S_s) \times L^2(\mathbb{R}) \to L^2(S_r) \times L^2(\mathbb{R})$ are the linear operators given by

$$\begin{aligned} (\tilde{F}\tilde{g})(\hat{x}, t) &:= \int_\Omega \int_{-\infty}^{t} \tilde{u}_\infty(\hat{x}, d, t - \tau)\, \tilde{g}(d, \tau)\, \mathrm{d}\tau\, \mathrm{d}s_d, \\ (\tilde{N}\tilde{g})(x, t) &:= \int_{S_s} \int_{-\infty}^{t} \tilde{u}(x, y, t - \tau)\, \tilde{g}(y, \tau)\, \mathrm{d}\tau\, \mathrm{d}s_y, \end{aligned} \tag{31}$$

where e.g. $\tilde{u}(x,y,t)$ is the scattered field due to u^i generated by an impulsive point source $\delta(x-y)\delta(t)$. To justify the claim of the domain and the range of $\tilde{F}$ and $\tilde{N}$, it is noted by way of the Plancherel identity and the compact frequency support of $g_z^{\mathcal{W}}$, see (29), that

$$\begin{aligned} \| \tilde{Q}\tilde{g}_z^{\mathcal{W}} \|_{L^2(\bullet)\times L^2(\mathbb{R})} &= 2 \| Q g_z^{\mathcal{W}} \|_{L^2(\bullet)\times L^2(\digamma_\omega)}, && \bullet \in \{\Omega, S_r\}, \quad Q \in \{F, N\} \\ \| \tilde{g}_z^{\mathcal{W}} \|_{L^2(\bullet)\times L^2(\mathbb{R})} &= 2 \| g_z^{\mathcal{W}} \|_{L^2(\bullet)\times L^2(\digamma_\omega)}, && \bullet \in \{\Omega, S_s\} \end{aligned} \tag{32}$$

where the norms on the right-hand sides are implicit to postulated frequency-domain mapping, see (31). By virtue of (29) and the second of (32), it is clear that the (weighted) *multi-frequency* indicator function (26) can be interpreted as that stemming from either of the *time-domain* linear sampling equations (30), i.e. that

$$\Pi^{(1)}_{\digamma,\mathcal{W}}(z) \;=\; \frac{1}{\| \tilde{g}_z^{\mathcal{W}} \|_{L^2(\bullet)\times L^2(\mathbb{R})}}.$$

It is recalled, however, that the above analogy is established under a severe limitation that $\omega_1 = 0$, i.e. that the observations of the time-harmonic scattered field are available down to zero frequency which is in practice never the case. Nonetheless, the featured example may help shed light on the relationship between the time- and frequency-domain treatments and, in situations where the featured quantities do not vary significantly over the "bottom" frequency range $[-\omega_1, \omega_1]$, augmented by suitable interpolation to establish the actual link.

4.2. "Parallel" indicator function

Another possible choice of a cumulative indicator function can be written as an L^2-norm of the "monochromatic" indicator over the featured frequency band, i.e.

$$\Pi^{(2)}_{\digamma}(z) := \left\| \frac{1}{\| g_z \|_{L^2(\bullet)}} \right\|_{L^2(\digamma_\omega)} = \left(\int_{\omega_1}^{\omega_2} \| g_z(\cdot,\omega) \|^{-2}_{L^2(\bullet)} \, \mathrm{d}\omega \right)^{1/2}, \quad \begin{cases} \bullet = \Omega & \text{(plane waves)}, \\ \bullet = S_s & \text{(point sources)}. \end{cases} \tag{33}$$

The reasoning behind proposition (33) is that of "constructive interference" where, again assuming that $\Lambda \cap \digamma_{k^2} = \emptyset$, distributions $1/\| g_z(\cdot,\omega) \|_{L^2(S_s)}$, $\omega \in \digamma_\omega$ reinforce each other in exposing the support of the scatterer by jointly vanishing when $z \in \mathbb{R}^3 \setminus D$.

To ensure the robustness of the multi-frequency reconstruction scheme, however, the critical issue with both (25) and (33) is their behavior and performance in situations when $\Lambda \cap \digamma_{k^2} \neq \emptyset$ – a possibility that cannot be discarded beforehand for the logical value of the latter inequality is, for given $\digamma_{k^2}$, dependent on the geometry and nature of a hidden scatterer. Given the fact that both $\Pi^{(1)}_{\digamma}$ and $\Pi^{(2)}_{\digamma}$ vanish when $z \notin D$ and $\Lambda \cap \digamma_{k^2} = \emptyset$, of particular concern here is the situation when $z \in D$ and $\digamma_{k^2}$ contains at least one eigenvalue of the relevant interior problem. Indeed, if either candidate for a cumulative indicator function necessarily vanishes in this case, such behavior would preclude its utility as a characteristic function of the support of the obstacle in a generic scattering environment.

4.3. Behavior of the solution in a neighborhood of an eigenvalue

To expose the utility of (band-limited) cumulative indicator functions proposed in Sections 4.1 and 4.2, it is critical to understand the behavior an approximate solution, g_z^ϵ, to the far-field equation (7) or its near-field counterpart (12) in the *neighborhood* of a "resonant" frequency ω_*, such that $\omega_*^2/c_\text{o}^2 = k_*^2 \in \Lambda$. In the context of far-field scattering, the first result in this direction was provided in [10] where it was shown that for $k^2 = k_*^2 \in \Lambda$ and almost every $z \in D$, Herglotz wave function $v_{g_{z,\delta}}^\epsilon$ (where $\epsilon = \epsilon(\delta)$ and $g_{z,\delta}^\epsilon$ is the Tikhonov-regularized solution of (22)) becomes unbounded, when $\delta \to 0$, in the $H^1(D)$-norm considering (2), and in the $L^2(D)$-norm considering (3). A similar result can be established for the unboundedness of the near-field potential $\vartheta_{g_z^\epsilon}$ as $\epsilon \to 0$, where g_z^ϵ satisfies (14). In the context of multi-frequency indicator functions (25) and (33), however, it is necessary to examine the *blow-up rate* of the relevant solution $g_{z,\epsilon}$ in the neighborhood of an eigenvalue $k_*^2 \in \Lambda$. Specifically, one needs to know whether $\|g_z(\cdot,\omega)\|_{L^2(\bullet)}$ is square-integrable with respect to ω over a given interval $[\omega_1, \omega_2]$, containing "resonant" frequency ω_* that corresponds to an eigenvalue of the germane interior problem.

Dirichlet obstacle. Starting with the case of a sound-soft obstacle, consider the interior Dirichlet problem of finding $v_z \in H^1(D)$ that satisfies (16), and let $\theta := \Psi(\cdot, z, k)\,\chi$ where χ is a C^∞ cutoff function equaling unity in a neighborhood of ∂D and zero in a neighborhood of z. In a weak form, (16) can be written for $\varphi := v_z - \theta \in H_0^1(D)$ as

$$A\varphi \,-\, k^2 B\varphi \;=\; -\,\ell_{z,k}, \tag{34}$$

see e.g. [7], Section 5.3, where $H_0^1(D)$ denotes the Hilbert space of all $u \in H^1(D)$ such that $u = 0$ on ∂D; invertible bounded operator $A : H_0^1(D) \to H_0^1(D)$ and compact bounded operator $B : H_0^1(D) \to H_0^1(D)$ are defined, with help of the Riesz representation theorem, as

$$(A\varphi, \psi)_{H^1(D)} = \int_D \nabla\varphi \cdot \nabla\overline{\psi}\,\mathrm{d}x, \qquad (B\varphi, \psi)_{H^1(D)} = \int_D \varphi\,\overline{\psi}\,\mathrm{d}x, \qquad \forall \psi \in H_0^1(D),$$

and

$$(\ell_{z,k}, \psi)_{H^1(D)} = \int_D \big(\nabla\theta \cdot \nabla\overline{\psi} - k^2\theta\,\overline{\psi}\big)\,\mathrm{d}x \qquad \forall \psi \in H_0^1(D). \tag{35}$$

For further reference, it is noted by virtue of (35) and the analyticity of $\Psi(\cdot, z, k)$ with respect to k that $\ell_{z,k}$ is continuous in k over any compact region in the complex plane.

Theorem 5. *Let k_*^2 be an isolated Dirichlet eigenvalue for $-\Delta$ in D, and consider $\alpha > 0$ such that the ball $\mathcal{B}_{k_*^2,\alpha} := \{k^2 : |k^2 - k_*^2| < \alpha,\, k^2 \neq k_*^2\}$ does not contain any eigenvalues other than k_*^2. Next, let g_z^ϵ be an approximate solution of either the far-field or the near-field equation, specified respectively in Lemma 2 and Lemma 1. Then for sufficiently small $\epsilon > 0$ and $\alpha > 0$, and almost every $z \in D$ one has*

$$\|v_{g_z^\epsilon}\|_{H^1(D)} \geqslant \frac{C_1}{|k^2 - k_*^2|} \quad \textit{and} \quad \|g_z^\epsilon\|_{L^2(\Omega)} \geqslant \frac{C_2}{|k^2 - k_*^2|} \quad \textit{(far-field observations)}, \tag{36}$$

and

$$\|\vartheta_{g_z^\epsilon}\|_{H^1(D)} \geqslant \frac{C_1}{|k^2-k_*^2|} \quad \textit{and} \quad \|g_z^\epsilon\|_{L^2(S_s)} \geqslant \frac{C_2}{|k^2-k_*^2|} \quad \textit{(near-field observations)} \tag{37}$$

for all $k^2 \in \mathcal{B}_{k_*^2,\alpha}$, where v_g and ϑ_g are given respectively by (11) and (15), while C_1 and C_2 are positive constants dependent on z, k_* and α, but not on k and ϵ.

Proof. Consider the compact self-adjoint operator $T := A^{-1/2}BA^{-1/2} : H_0^1(D) \to H_0^1(D)$, and set $\xi := 1/k^2$ (note that $A^{1/2}$ is defined via spectral decomposition since A is self-adjoint and positive definite). Obviously, $\lambda_* := 1/k_*^2$ is an isolated eigenvalue for T. To facilitate the ensuing discussion, let E_{λ_*} denote the eigenspace of T corresponding to λ_*, and let $M_{\lambda_*} \supseteq E_{\lambda_*}$ denote the *generalized* eigenspace of T associated with λ_* that is spanned by the functions $w_* \in H_0^1(D)$ for which $(T-\lambda_* I)^p w_* = 0,\ p \geqslant 1$. In this setting it can be shown (see [23], p. 180), that the resolvent $R(\xi) := (T-\xi I)^{-1}$ of compact operator T admits the Laurent series expansion

$$R(\xi) \ = \ -\frac{P}{(\xi-\lambda_*)} - \sum_{p=1}^{\infty} \frac{Q^p}{(\xi-\lambda_*)^{p+1}} + \sum_{p=0}^{\infty} (\xi-\lambda_*)^p S^{p+1} \tag{38}$$

in a neighborhood of λ_*, where $P : H_0^1(D) \to M_{\lambda_*}$ is the orthogonal projection onto the generalized eigenspace of T corresponding to λ_*, bounded operator $Q = (T-\lambda_* I)P$ is the so-called eigen-nilpotent projection satisfying $Q = PQ = QP$, and S is a bounded operator satisfying $(T-\lambda_* I)S = I - P$ such that $SP = PS = 0$. By virtue of the compactness of T, $Q^p = 0$ for $p \geqslant m_* \geqslant 1$ where (finite integer) $m_* = \dim M_{\lambda_*}$, which reduces the principal part of the Laurent series to a finite sum. Thus, without loss of generality one can choose an orthonormal basis in M_{λ_*}. One may also note that the range of Q^{m_*-1} is contained in the eigenspace E_{λ_*} of T since $(T-\lambda_* I)Q^{m_*-1} = Q^{m_*} = 0$. If k^2 is not a Dirichlet eigenvalue for D, (34) requires that $\varphi := v_z - \theta$ satisfies $k^2(T-\xi I)A^{1/2}\varphi = A^{-1/2}\ell_{z,k}$ whereby $k^2 A^{1/2}\varphi = R(\xi)A^{-1/2}\ell_{z,k}$ i.e.

$$k^2 A^{1/2}\varphi \ = \ -\frac{PA^{-1/2}\ell_{z,k}}{(\xi-\lambda_*)} - \sum_{p=1}^{m_*-1} \frac{Q^p A^{-1/2}\ell_{z,k}}{(\xi-\lambda_*)^{p+1}} + \sum_{p=0}^{\infty} (\xi-\lambda_*)^p S^{p+1} A^{-1/2}\ell_{z,k}.$$

Thus

$$\begin{aligned} \|k^2 A^{1/2}\varphi\| \ &= \ \frac{1}{(\xi-\lambda_*)^{m^*}} \Bigg\| Q^{m_*-1}A^{-1/2}\ell_{z,k} + \sum_{p=1}^{m_*-2} (\xi-\lambda_*)^{m_*-p-1} Q^p A^{-1/2}\ell_{z,k} \\ &\quad + \ (\xi-\lambda_*)^{m_*-1} PA^{-1/2}\ell_{z,k} - \sum_{p=0}^{\infty} (\xi-\lambda_*)^{p+m_*} S^{p+1} A^{-1/2}\ell_{z,k} \Bigg\| \end{aligned} \tag{39}$$

Substituting $\xi := 1/k^2$ ($k^2 \in \mathcal{B}_{k_*^2,\alpha}$) and $\lambda_* := 1/k_*^2$ in (39), it further follows from i) the reverse triangle inequality, ii) the facts that A, Q and S are bounded operators and iii) the fact that $\ell_{z,k}$ is uniformly bounded, that for α sufficiently small

$$\|k^2 A^{1/2}\varphi\|_{H^1(D)} \ \geqslant \ \frac{|k^2 k_*^2|^{m_*}}{|k^2-k_*^2|^{m_*}} \|Q^{m_*-1}A^{-1/2}\ell_{z,k}\|_{H^1(D)} - C_p, \tag{40}$$

where $C_p \geqslant 0$ depends on z and k_*, but not on k. With this result in place, it suffices to show that $Q^{m_*-1}A^{-1/2}\ell_{z,k_*} \neq 0$ for almost all $z \in D$. Indeed, if this is the case then by the continuity argument one finds that $\|Q^{m_*-1}A^{-1/2}\ell_{z,k}\| \geqslant \frac{1}{2}\|Q^{m_*-1}A^{-1/2}\ell_{z,k_*}\|$ for $k^2 \in \mathcal{B}_{k_*^2,\alpha}$ and sufficiently small $\alpha > 0$, whereby

$$\|k^2 A^{1/2}\varphi\|_{H^1(D)} \;\geqslant\; \frac{|k^2 k_*^2|^{m_*}}{2|k^2 - k_*^2|^{m_*}}\,\|Q^{m_*-1}A^{-1/2}\ell_{z,k_*}\|_{H^1(D)} \;-\; C_p, \qquad m_* \geqslant 1. \tag{41}$$

Now assuming the contrary i.e. that $Q^{m_*-1}A^{-1/2}\ell_{z,k_*} = 0$, one finds that $A^{-1/2}\ell_{z,k_*}$ is orthogonal to at least one eigenvector, hereon denoted by u_*, in E_{λ_*}. Owing to the fact that operator $A^{-1/2}$ is self-adjoint, this implies

$$(\ell_{z,k_*}, A^{-1/2}u_*) = 0, \quad \text{where} \quad (I \,-\, k_*^2\, A^{-1/2}BA^{-1/2})u_* = 0,$$
$$\text{i.e.} \quad A^{-1/2}(A - k_*^2 B)A^{-1/2}u_* = 0.$$

By the bijectivity of $A^{-1/2}$, this result in turn requires that ℓ_{z,k_*} be orthogonal to an element in the kernel of $A - k_*^2 B$, i.e. that ℓ_{z,k_*} is orthogonal to an eigenfunction corresponding to Dirichlet eigenvalue k_*^2. Letting ϕ_* denote this Dirichlet eigenfunction, the use of (35) and the first Green's identity demonstrates that

$$0 \;=\; (\ell_{z,k_*}, \phi_*)_{H^1(D)} = \int_D \left(\nabla\theta \cdot \nabla\overline{\phi}_* - k_*^2\,\theta\,\overline{\phi}_*\right) \mathrm{d}x \;=\; \int_{\partial D} (\overline{\phi}_*)_{,\nu}\, \Psi(x, z, k_*)\, \mathrm{d}s_x,$$

for $z \in D$. By virtue of the the symmetry of Ψ with respect to its first two arguments, one consequently finds that

$$w(z) := \int_{\partial D} (\overline{\phi}_*)_{,\nu}\, \Psi(z, x, k_*)\, \mathrm{d}s_x = 0,$$

Since $w(z) = 0$ for $z \in \mathcal{Z} \subset D$ such that $\mathcal{Z}$ has nonzero measure it follows, by virtue of unique continuation applied to $w(z)$ which solves the Helmholtz equation, that $w(z) = 0$ in D and thus $w(z) = 0$ on ∂D by the continuity of single-layer potentials. The latter result implies that $w = 0$ in $\mathbb{R}^3 \setminus \overline{D}$ as a radiating solution to the exterior Dirichlet problem with zero boundary data, which in turn requires that $\partial\phi_*/\partial\nu = 0$ on ∂D since $w = 0$ everywhere. In light of the Holmgren's uniqueness theorem and the fact that $\phi_* = 0$ on ∂D, one concludes that $\phi_* = 0$ in D which contradicts the premise that ϕ_* is an eigenfunction.

Since C_p in (40) behaves as $O(1)$ with diminishing α, (41) implies that

$$\|A^{1/2}\varphi\|_{H^1(D)} \;\geqslant\; \frac{C}{|k^2 - k_*^2|}\|Q^{m_*-1}A^{-1/2}\ell_{z,k_*}\|_{H^1(D)}$$

for $k^2 \in \mathcal{B}_{k_*^2,\alpha}$ and sufficiently small α, where C is a positive constant independent of k such that $0 < C < \frac{1}{2}|k^2 k_*^2|^{m_*}\ \ \forall k^2 \in \mathcal{B}_{k_*^2,\alpha}$. Since i) $A^{-1/2}$ and Q are both bounded operators; ii) ℓ_{z,k_*} is finite; iii) χ vanishes in a neighborhood of z; and iv) $Q^{m_*-1}A^{-1/2}\ell_{z,k_*} \neq 0,\ q \geqslant 0$ for almost all $z \in D$, the above inequality implies that

$$\|v_z\|_{H^1(D)} \geqslant \left|\|\varphi\|_{H^1(D)} - \|\Psi(\cdot, z, k)\chi(\cdot)\|_{H^1(D)}\right| \geqslant \frac{C'}{|k^2 - k_*^2|} - C'' \geqslant \frac{C'''}{|k^2 - k_*^2|}$$

for suitably chosen constant $C'''>0$ dependent on z, k_* and α, but not on k. Next, let g_z^ϵ be the approximate solution to either the far-field or the near-field equation provided, respectively, by Lemma 2 and Lemma 1. These lemmas stipulate that the Herglotz wave function $v_{g_z^\epsilon}$ given by (11) and the single-layer potential $\vartheta_{g_z^\epsilon}$ given by (15) converge to v_z in the $H^1(D)$ norm as $\epsilon \to 0$ uniformly for $k^2 \in \mathcal{B}_{k_*^2,\alpha}$. Thus, for sufficiently small $\epsilon > 0$, $v_{g_z^\epsilon}$ and $\vartheta_{g_z^\epsilon}$ inherit the behavior of v_z i.e

$$\|v_{g_z^\epsilon}\|_{H^1(D)} \geqslant \frac{C_1'}{|k^2-k_*^2|} \qquad \text{and} \qquad \|\vartheta_{g_z^\epsilon}\|_{H^1(D)} \geqslant \frac{C_2'}{|k^2-k_*^2|}$$

where C_1' and C_2' are positive constants independent of k and ϵ. With this result in place, the claim of the theorem is established by way of estimates

$$\|g_z^\epsilon\|_{L^2(\Omega)} \geqslant C_1''\,\|v_{g_z^\epsilon}\|_{H^1(D)} \geqslant \frac{C_1}{|k^2-k_*^2|} \quad \text{and} \quad \|g_z^\epsilon\|_{L^2(S_c)} \geqslant C_2''\,\|\varphi_{g_z^\epsilon}\|_{H^1(D)} \geqslant \frac{C_2}{|k^2-k_*^2|},$$

where $C_1 = C_1'C_1''$ and $C_2 = C_2'C_2''$ are positive constants dependent on z, k_* and α, but not on k and ϵ. □

Penetrable obstacle. Next, consider the interior transmission problem of finding $v_z \in L^2(D)$ and $w_z \in L^2(D)$ solving (19) so that $u_z = w_z - v_z \in H^2(D)$. Analogous to the treatment of the Dirichlet problem, let $\theta := \Psi(\cdot,z,k)\chi$ where χ is a C^∞ cut-off function equaling unity in a neighborhood of ∂D, and vanishing in a neighborhood of $z \in D$. To facilitate the analysis, it is hereon assumed that $n(x)$ is real-valued such that $n > 1+\delta_n$ in D for some constant $\delta_n > 0$ (the case of when $n < 1-\delta_n$ can be handled in exactly the same way). The reason for this restriction resides in the fact that the analytical framework for dealing with the transmission eigenvalue problem corresponding to complex-valued n, which entails complex eigenvalues k^2, is not yet completely developed, see e.g.[3, 8].

Following [40, 11], one can show that (19) can be written as a fourth-order equation in terms of $u_z \in H^2(D)$, namely

$$\left(\Delta + k^2\right) \frac{1}{n-1} \left(\Delta + k^2 n\right) u_z \;=\; 0 \qquad \text{in} \quad D, \tag{42}$$

that is accompanied by the boundary conditions $u_z = \Psi(\cdot,z,k)$ and $(u_z)_{,\nu} = \Psi_{,\nu}(\cdot,z,k)$ on ∂D. In what follows, let $H_0^2(D)$ denote the Hilbert space of all $u \in H^2(D)$ such that $u = 0$ and $u_{,\nu} = 0$ on ∂D. In this setting, the variational form of (42) can be written in terms of $v := u_z - \theta \in H_0^2(D)$ as

$$\int_D \frac{1}{n-1}(\Delta v + k^2 n\, v)(\Delta\overline{\psi} + k^2\overline{\psi})\,\mathrm{d}x = -\int_D \frac{1}{n-1}(\Delta\theta + k^2 n\,\theta)(\Delta\overline{\psi} + k^2\overline{\psi})\,\mathrm{d}x \quad \forall \psi \in H_0^2(D),$$

i.e.

$$Av \;-\; k^2 B_1 v \;+\; k^4 B_2 v \;=\; -\ell_{z,k}. \tag{43}$$

Here $A : H_0^2(D) \to H_0^2(D)$ is a bounded, positive definite self-adjoint operator given by

$$(A\varphi,\psi)_{H^2(D)} = \int_D \frac{1}{n-1}\Delta\varphi\,\Delta\overline{\psi}\,\mathrm{d}x,$$

(note that the $H^2(D)$ norm of a field with zero Cauchy data on ∂D is equivalent to the $L^2(D)$ norm of its Laplacian); $B_1 : H_0^2(D) \to H_0^2(D)$ and $B_2 : H_0^2(D) \to H_0^2(D)$ are compact bounded operators such that

$$(B_1\varphi, \psi)_{H^2(D)} \;=\; -\int_D \frac{1}{n-1}\left(\Delta\varphi\,\overline{\psi} + \varphi\,\Delta\overline{\psi}\right)\,\mathrm{d}x \;-\; \int_D \varphi\,\Delta\overline{\psi}\,\mathrm{d}x,$$
$$(B_2\varphi, \psi)_{H^2(D)} \;=\; \int_D \frac{n}{n-1}\varphi\,\overline{\psi}\,\mathrm{d}x,$$

and

$$(\ell_{z,k}, \psi)_{H^2(D)} \;=\; \int_D \frac{1}{n-1}(\Delta\theta + k^2 n\,\theta)(\Delta\overline{\psi} + k^2\overline{\psi})\,\mathrm{d}x, \quad \forall\psi \in H_0^2(D).$$

Theorem 6. *Let k_*^2 be an isolated transmission eigenvalue, and consider $\alpha > 0$ such that the ball $\mathcal{B}_{k_*^2,\alpha} := \{k^2 : |k^2 - k_*^2| < \alpha,\ k^2 \neq k_*^2\}$ does not contain any eigenvalues other than k_*^2. Further, let g_z^ϵ be the approximate solution of either the far-field or the near-field equation, specified respectively in Lemma 3 and Lemma 4. Then for sufficiently small $\epsilon > 0$ and $\alpha > 0$, and almost every $z \in D$ one has*

$$\|v_{g_z^\epsilon}\|_{L^2(D)} \geqslant \frac{C_1}{|k^2 - k_*^2|} \quad \textit{and} \quad \|g_z^\epsilon\|_{L^2(\Omega)} \geqslant \frac{C_2}{|k^2 - k_*^2|} \quad \textit{(far-field observations)}, \tag{44}$$

and

$$\|\vartheta_{g_z^\epsilon}\|_{L^2(D)} \geqslant \frac{C_1}{|k^2 - k_*^2|} \quad \textit{and} \quad \|g_z^\epsilon\|_{L^2(S_s)} \geqslant \frac{C_2}{|k^2 - k_*^2|} \quad \textit{(near-field observations)} \tag{45}$$

for all $k^2 \in \mathcal{B}_{k_*^2,\alpha}$, where v_g and ϑ_g are given respectively by (11) and (15), while C_1 and C_2 are positive constants dependent on z, k_* and α, but not on k and ϵ.

Proof. Let $v_B := k^2 B_2^{1/2} v$ (note that $B_2^{1/2}$ is defined via spectral decomposition for B_2 is positive semi-definite), and let $T : H_0^2(D) \times H_0^2(D) \to H_0^2(D) \times H_0^2(D)$ be a compact operator given by

$$T := \begin{pmatrix} A^{-1/2} B_1 A^{-1/2} & -A^{-1/2} B_2^{1/2} A^{-1/2} \\ A^{1/2} B_2^{1/2} A^{-1/2} & 0 \end{pmatrix}. \tag{46}$$

In light of the relationship

$$A^{1/2}\big(I - k^2 A^{-1/2} B_1 A^{-1/2} + k^4 A^{-1/2} B_2 A^{-1/2}\big)\, A^{1/2} v \;=\; -\ell_{z,k},$$

(46) permits (43) to be rewritten as

$$k^2\big(T - \xi I\big) A^{1/2}\varphi \;=\; A^{-1/2} l_{z,k}, \qquad \varphi = \begin{pmatrix} v \\ v_B \end{pmatrix}, \qquad l_{z,k} = \begin{pmatrix} \ell_{z,k} \\ 0 \end{pmatrix},$$

where $\xi := 1/k^2$. This transformation allows the resolvent of (46), namely $R(\xi) = (T - \xi I)^{-1}$, to be treated in the way analogous to that in Theorem 5. As a result, one finds that

$$\|A^{1/2}\varphi\|_{H^2(D)} \;\geqslant\; \frac{C}{|k^2 - k_*^2|}\|Q^{m_*-1} A^{-1/2} l_{z,k_*}\|_{H^2(D)}$$

for $k^2 \in \mathcal{B}_{k_*^2,\alpha}$, where $0<C<1$ is independent of k, and $Q^{m_*-1}: H_0^2(D)\times H_0^2(D) \to E_{\lambda_*}$ is the projection to the eigenspace of (46) corresponding to $\lambda_* := 1/k_*^2$. Now it remains to show that $Q^{m_*-1}A^{-1/2}l_{z,k_*} \neq 0$ for almost all $z \in D$. Again, assuming the contrary i.e. that $Q^{m_*-1}A^{-1/2}l_{z,k_*} = 0$ over $\mathcal{Z} \subset D$ with non-zero measure for $k^2 \in \mathcal{B}_{k_*^2,\alpha}$, it follows as in Theorem 5 that $l_{z,k_*} \in H_0^2(D)$ is orthogonal to an element in the kernel of $A - k_*^2 B_1 + k_*^4 B_2$ which is a transmission eigenfunction corresponding to λ_*. On letting ϕ_* denote this eigenfunction, one has

$$0 \;=\; (l_{z,k_*}, \phi_*)_{H^2(D)} \;=\; \int_D \frac{1}{n-1}(\Delta\theta + k_*^2 n\,\theta)(\Delta\overline{\phi}_* + k_*^2\overline{\phi}_*)\,\mathrm{d}x. \tag{47}$$

Integration of (47) by parts yields

$$\int_{\partial D} \frac{1}{n-1}(\Delta + k_*^2 n)\overline{\phi}_*\; \Psi_{,\nu}(x,z,k_*)\,\mathrm{d}s_x - \int_{\partial D}\Big(\frac{1}{n-1}(\Delta + k_*^2 n)\overline{\phi}_*\Big)_{,\nu}\Psi(x,z,k_*)\,\mathrm{d}s_x \;=\; 0, \tag{48}$$

by virtue of the definition of ϕ_* and the boundary conditions imposed on $\theta := \Psi\chi$, where the two integrals are understood in the sense of $H^{\mp 1/2}$ resp. $H^{\mp 3/2}$ duality pairing. On setting

$$w \;:=\; \frac{1}{n-1}(\Delta + k_*^2 n)\overline{\phi}_* \tag{49}$$

which satisfies the Helmholtz equation in D (recall that n is real-valued), one finds via the Green's representation theorem that

$$w(z) = \int_{\partial D}\Big(w(x)\,\Psi_{,\nu}(z,x,k_*) \;-\; w_{,\nu}(x)\,\Psi(z,x,k_*)\Big)\,\mathrm{d}s_x \qquad \text{for } z \in D. \tag{50}$$

On the basis of (48) which applies over $\mathcal{Z} \subset D$, (50), the symmetry of Ψ with respect to its first two arguments, and the unique continuation principle, it follows that $w = 0$ in D. By virtue of (49), ϕ_* solves the Helmholtz equation in D with zero Cauchy data since $\phi_* \in H_0^2(D)$. As a result one finds, again exercising unique continuation, that $\phi_* = 0$ in D which contradicts the premise that ϕ_* is an eigenfunction. Proceeding with the proof as in the case of a Dirichlet obstacle and employing the fact that B_2 is bounded, one finds that for almost all $z \in D$ and $|k_*^2 - k^2| < \alpha$

$$\|w_z - v_z\|_{H^2(D)} \;=\; \|u_z\|_{H^2(D)} \;\geqslant\; \frac{C'}{|k^2 - k_*^2|},$$

for sufficiently small $\alpha > 0$ and some $C' > 0$ dependent on z, k_* and α, but not on k. By making an appeal to the well-posedness of (20) as in Lemma 1, one finally obtains the estimate

$$\|v_z\|_{L^2(D)} \;\geqslant\; C''\|u_z\|_{H^2(D)} \;\geqslant\; \frac{C'''}{|k^2 - k_*^2|}$$

for suitably chosen $C'' > 0$ and $C''' > 0$ dependent on z, k_* and α, but not on k. With this result in place, the convergence of $v_{g_z^\epsilon}$ (in the case of far-field observations) and $\vartheta_{g_z^\epsilon}$ (in the case of near-field observations) to v_z in the $L^2(D)$-norm as $\epsilon \to 0$, stipulated respectively in Lemma 3 and Lemma 4, completes the proof of (44) and (45) as in Theorem 5. $\square$

Remark 2. As a follow-up to the discussion in Section 3.2 it is noted that, in the case of far-field measurements, it is possible to extend the results of Theorem 5 and Theorem 6 to Tikhonov-regularized solution (22) of the far-field equation.

Remark 3. For penetrable obstacles, it is further feasible to remove the assumption that the mass density ρ is constant throughout the system and to consider a generalization of (3), where $\rho = \rho(x)$ inside the obstacle while maintaining $\rho = \rho_o = \text{const.}$ in $\mathbb{R}^3 \backslash \overline{D}$. For this configuration, the relevant scattering problem can be written as

$$\begin{aligned} \Delta u + k^2 u = 0 \qquad & \text{in} \quad \mathbb{R}^3 \setminus \overline{D}, \\ \Delta \varpi + k^2 n\, \varpi = 0 \qquad & \text{in} \quad D, \\ \varpi - u = u^i, \quad \beta \varpi_{,\nu} - u_{,\nu} = u^i_{,\nu} \qquad & \text{on} \quad \partial D, \\ \lim_{|x| \to \infty} |x| \left(\frac{\partial u}{\partial |x|} - \mathrm{i} k u \right) = 0, & \end{aligned} \tag{51}$$

where $\beta = \rho_o / \rho$ and $\rho(x)$ is, similar to the hypothesis on $n(x)$, assumed to be "slowly" varying so that the term containing $\nabla \rho$ can be omitted from the field equation. By making reference to the existing studies of the affiliated interior transmission problem [9, 13], the claims of Section 3.1 can be extended verbatim to this more general configuration. A commensurate extension of the results obtained in Section 4.3 is, however, fairly involved and entails additional assumptions on β and n employed by the analysis of the featured interior transmission problem.

Remark 4. From Theorem 5 and Theorem 6, it is clear that $\|g_z^\epsilon\|_{L^2(\bullet)}$, $\bullet = \Omega, S_s$ behaves as $O(|\omega - \omega_*|^{-m})$, $m \geqslant 1$ when $\omega \to \omega_* = c_o\, k_*$. As a result, the multi-frequency solution density g_z^ϵ featured in (25) and (33) does not belong to $L^2(\bullet) \times L^2(\digamma_\omega)$ when the relevant interior problem over D is characterized by eigenvalues k_*^2 such that $\omega_* = c_o\, k_* \in \digamma_\omega$. In light of this result it is noted that "serial" indicator function (25), in contrast to its "parallel" companion (33), is not applicable to such configurations – a finding that is illustrated in the sequel.

5. Results

In what follows, an attempt at multi-frequency obstacle reconstruction via the linear sampling method is made for two sample configurations, namely that entailing far-field scattering by a unit ball in $\mathbb{R}^3$ – a problem investigated analytically, and an affiliated far-field problem for a square scatterer in $\mathbb{R}^2$ **[?]** which exposes the performance of the method in a generic computational setting. With regard to the latter example, it is noted that both the claim and the structure of the proof of Theorem 5 and Theorem 6 is independent of the dimensionality of the problem, and could be extended to scattering in $\mathbb{R}^2$ by invoking the two-dimensional counterparts of Lemmas 1-4 (see, e.g. [7]). For the brevity of exposition, however, the treatment of the two-dimensional case is in this study limited to a numerical example.

5.1. Analytical study: spherical scatterer in $\mathbb{R}^3$

To shed light on the foregoing developments, consider the scattering of plane waves by a *unit ball* D, centered at the origin so that $\partial D = \{x \in \mathbb{R}^3 : \ |x| = 1\}$. Assuming both the obstacle and the background to be non-dissipative, the remainder of this study focuses on the existence of real-valued eigenvalues characterizing the associated interior (Dirichlet or transmission) problem, and their effect on indicator functions (25) and (33), in the context of the *far-field* formulation (7) of the linear sampling method. For a unified analytical and computational treatment, the reference is hereon made to the generalized scattering problem (51) which permits the Dirichlet case (2) and penetrable case (3) to be recovered by setting respectively $\beta \to \infty$ and $\beta = 1$.

Far-field pattern. Assuming the incident field u^i to be in the form of a plane wave as in (1a), u and ϖ solving (51) can be expanded over the set of spherical harmonics, $(Y_p^m)_{p\in\mathbb{N}_0, m\in\{-p,\ldots,p\}}$, as

$$\begin{aligned} u(x,d) &= \sum_{p=0}^{\infty} \sum_{m=-p}^{p} \lambda_p^m(d)\, h_p^{(1)}(k|x|)\, Y_p^m(\hat{x}), \quad x \in \mathbb{R}^3\backslash D, \quad d \in \Omega, \\ \varpi_(x,d) &= \sum_{p=0}^{\infty} \sum_{m=-p}^{p} \mu_p^m(d)\, j_p(\gamma k|x|)\, Y_p^m(\hat{x}), \quad x \in D, \quad d \in \Omega, \end{aligned} \tag{52}$$

where $\mathbb{N}_0$ is the set of all non-negative integers; $\gamma = \sqrt{n} = c_o/c$; λ_p^m and μ_p^m are, for fixed k and d, constants dependent only on their indexes, and j_p and $h_p^{(1)}$ denote respectively the pTh-order spherical Bessel and Hankel functions of the first kind. On employing the boundary conditions over the unit sphere ∂D and the orthonormality of spherical harmonics, the solution for the scattered field in $\mathbb{R}^3\backslash D$ can be found as

$$u(x,d) = \sum_{p=0}^{\infty} \mathrm{i}^p (2p+1)\, \Theta_p(k)\, h_p^{(1)}(k|x|)\, P_p(\hat{x}\cdot d), \qquad \Theta_p(k) = \frac{j_p'(k) - \alpha_p j_p(k)}{\alpha_p h_p^{(1)}(k) - h_p^{(1)'}(k)}, \tag{53}$$

where P_p denotes the pth-order Legendre polynomial; f' is the derivative of f with respect to its argument, and

$$\alpha_p(k) \ = \ \beta\, \gamma\, \frac{j_p'(\gamma k)}{j_p(\gamma k)} \tag{54}$$

signifies an effective admittance of surface ∂D at wavenumber k and pth spherical harmonic. Here it is noted that (53) is well behaved since the denominator $\alpha_p h_p^{(1)} - h_p^{(1)'}$ does not vanish when $k \in \mathbb{R}^+$ and $p \in \mathbb{N}_0$, see also [15] for a similar argument in electromagnetism. Indeed, by assuming the contrary one finds via Nicholson's formula that

$$\alpha_p(k) |h_p^{(1)}(k)|^2 \ - \ h_p^{(1)'}(k) \overline{h_p^{(1)}}(k) \ = \ 0, \tag{55}$$

which guarantees that $h_p^{(1)}(k) \neq 0$ for $k \in \mathbb{R}^+$. The imaginary part of (55) requires that the Wronskian $W(j_p(k), y_p(k)) = j_p(k) y_p'(k) - j_p'(k) y_p(k)$, involving spherical Bessel functions

of the first and second kind, vanishes when $k \in \mathbb{R}^+$. But this cannot hold owing to the identity

$$W(j_p(k), y_p(k)) \;=\; \frac{1}{k^2}, \tag{56}$$

see e.g. [18].

By way of (53) and Theorem 2.15 in [18], the scattered far-field pattern generated by the plane waves impinging on a unit ball centered at the origin can be computed as

$$u_\infty(\hat{x}, d) \;=\; \sum_{p=0}^{\infty} \frac{(2p+1)}{\mathrm{i}k}\, \Theta_p(k)\, P_p(\hat{x}\cdot d), \tag{57}$$

which can be used to compute the far-field variation of a solution to both (2), by setting $\beta \to \infty$, and (3) by taking $\beta = 1$. In the former case, one in particular finds that

$$\Theta_p(k) = -\frac{j_p(k)}{h_p^{(1)}(k)}. \tag{58}$$

Interior problem. As examined in Section 3.1, the solvability of integral equation (7) in the far-field formulation of the method hinges on the uniqueness of a solution to the corresponding interior problem. With reference to the "unifying" scattering problem (51), one can in particular show following the approach exercised earlier that the associated far-field operator $F : L^2(\Omega) \to L^2(\Omega)$, given by (8), is injective with dense range if and only if there does not exist a Herglotz wave function v_g of form (11) with non-zero density $g \in L^2(\Omega)$ such that pair (v_g, w) solves the homogeneous interior transmission problem

$$\begin{aligned} \Delta v_g + k^2 v_g &= 0 \qquad && \text{in} \quad D, \\ \Delta w + k^2 n\, w &= 0 \qquad && \text{in} \quad D, \\ v_g = w, \quad (v_g)_{,\nu} &= \beta\, w_{,\nu} \qquad && \text{on} \quad \partial D. \end{aligned} \tag{59}$$

On seeking the solution to (59) in terms of spherical harmonics

$$\begin{aligned} v_g(x) \;&=\; \sum_{p=0}^{\infty} \sum_{m=-p}^{p} v_p^m\, j_p(k|x|)\, Y_p^m(\hat{x}), \qquad x \in D, \\ w(x) \;&=\; \sum_{p=0}^{\infty} \sum_{m=-p}^{p} w_p^m\, j_p(\gamma k|x|)\, Y_p^m(\hat{x}), \quad x \in D, \end{aligned} \tag{60}$$

and employing the Funk-Hecke formula

$$\int_\Omega e^{-\mathrm{i}kx\cdot d}\, Y_p^m(d)\, \mathrm{d}s_d \;=\; \frac{4\pi}{i^p}\, j_p(k|x|)\, Y_p^m(\hat{x}), \qquad \forall x \in \mathbb{R}^3, \quad p \in \mathbb{N}_0, \quad m \in \{-p, \ldots, p\},$$

one finds that v_g, as given by (60a), is indeed a Herglotz wave function in the sense of (11). With such result in place, it can next be shown by exercising the homogeneous boundary conditions over ∂D in terms of (60) that a non-trivial solution to (59) exists if and only if there are values $k \in \mathbb{R}$ such that

$$j'_{p_\star}(k) - \alpha_{p_\star}(k)\, j_{p_\star}(k) \;=\; 0, \qquad p_\star \in \mathbb{N}_0, \tag{61}$$

where $\alpha_{p_\star}$ is defined via (54). From (61), it is in particular useful to note that $\Theta_{p_\star}(k)=0$ in the context of the scattered-field solution (53). As a result, the set of transmission eigenvalues characterizing (59) can be written as

$$\Lambda \;=\; \left\{k^2\colon \Theta_{p_\star}(k)=0,\; p_\star\in\mathbb{N}_0\right\}. \tag{62}$$

In the case of a Dirichlet obstacle ($\beta\to\infty$), (62) reduces to

$$\Lambda \;=\; \left\{k^2\colon j_{p_\star}(k)=0,\; p_\star\in\mathbb{N}_0\right\}. \tag{63}$$

Indicator functions. With reference to (7) and spherical-harmonics expansion (57) of u_∞, the far-field pattern of the fundamental solution Ψ can be computed as

$$\Psi_\infty(\hat{x},z,k) \;=\; \frac{1}{4\pi}e^{-\mathrm{i}k\hat{x}\cdot z} \;=\; \sum_{p=0}^{\infty}\sum_{m=-p}^{p}\mathrm{i}^{-p}\,j_p(k|z|)\,\overline{Y_p^m}(\hat{z})\,Y_p^m(\hat{x}). \tag{64}$$

As a result the source density g_z, solving (7) at a given sampling point $z\in\mathbb{R}^3$, is sought in the form

$$g_z(d) \;=\; \sum_{p=0}^{\infty}\sum_{m=-p}^{p} g_p^m\,Y_p^m(d), \qquad d\in\Omega \tag{65}$$

which, on substitution, yields

$$g_z(d) \;=\; \frac{k}{(4\pi)^2}\sum_{p=0}^{\infty}\frac{(2p+1)}{\mathrm{i}^{p-1}\Theta_p(k)}\,j_p(k|z|)\,P_p(\hat{z}\cdot d), \qquad d\in\Omega, \tag{66}$$

provided that the condition

$$\Theta_p(k)\neq 0, \qquad p\in\mathbb{N}_0$$

is met, i.e. that k^2 is not an eigenvalue of the interior problem (59). Unfortunately, series (66) does not belong to $L^2(\Omega)$ for any $k\in\mathbb{R}^+$ owing to the fact that its norm is given by

$$\|g_z\|^2_{L^2(\Omega)} \;=\; \frac{k^2}{(4\pi)^3}\sum_{p=0}^{\infty}\frac{(2p+1)}{|\Theta_p(k)|^2}\,j_p(k|z|)^2, \tag{67}$$

where the featured spherical (Bessel and Hankel) functions behave asymptotically such that

$$\frac{(2p+1)}{|\Theta_p(k)|^2}\,j_p(k|z|)^2 \;=\; \frac{4}{k^2}\left(\frac{1+\beta}{1-\beta}\right)^2\left(\frac{2|z|}{e\,k}\right)^{2p}p^{2p+1}\left(1+O(p^{-1})\right) \qquad \text{as} \quad p\to\infty, \tag{68}$$

see e.g. [18]. Indeed from (67) and (68), it is clear that

$$\|g_z\|_{L^2(\Omega)}=\infty, \qquad z\in\mathbb{R}^3\backslash\{0\}.$$

This result is not surprising since the far-field operator F is known to be compact with eigenvalues

$$\sigma_p \;=\; \frac{4\pi}{ik}\,\Theta_p(k), \qquad p\in\mathbb{N}_0, \tag{69}$$

that have the asymptotic behavior

$$\sigma_p \;=\; \pi\left(\frac{1-\beta}{1+\beta}\right)\left(\frac{e\,k}{2}\right)^{2p}\frac{1}{p^{2p+1}}\left(1+O(p^{-1})\right)\qquad\text{as}\quad p\to\infty, \tag{70}$$

and thus accumulate at zero. The blow-off feature of $\|g_z\|_{L^2(\Omega)}$ in $\mathbb{R}^3\backslash\{0\}$ can therefore be attributed to the smallest eigenvalues of the far-field operator. For practical purposes, however, this behavior can be regularized by truncating the spectrum of F "from below" at sufficiently small eigenvalues [15], i.e. by seeking a solution to the far-field equation (7) within a manifold

$$\text{span}\big(Y_p^m,\ p\in\{0,\ldots,N_t\},\ m\in\{-p,\ldots,p\}\big)\,,\qquad N_t<\infty.$$

With the above results in place, indicator functions (25) and (33), cumulative over $\mathit{\Gamma}_\omega=[\omega_1,\omega_2]$, can now be approximated by evaluating (67) up to truncation level N_t and employing piecewise-constant approximation of $g_z(\cdot,\omega)$ over a discrete set of *sampling frequencies*

$$\mathit{\Gamma}_\omega^h=\big\{\omega_1^s,\omega_2^s,\ldots\omega_{N_h}^s\big\}\subset\mathit{\Gamma}_\omega,\quad \omega_1^s{=}\omega_1,\quad \omega_{N_h}^s{=}\,\omega_2,\quad \omega_{m+1}^s{-}\omega_m^s=O(h){>}0,\quad m\in\{1,\ldots N_h\}$$

where h is the chosen level of discretization. Accordingly, one finds that

$$\check{\Pi}_{\mathit{\Gamma}}^{(1)}(z)\;=\;(4\pi)^{3/2}\left(\sum_{k\in\mathit{\Gamma}_k^h}\sum_{p=0}^{N_t}\frac{(2p+1)k^2}{|\Theta_p(k)|^2}\,j_p(k|z|)^2\right)^{-1/2} \tag{71}$$

and

$$\check{\Pi}_{\mathit{\Gamma}}^{(2)}(z)\;=\;(4\pi)^{3/2}\left(\sum_{k\in\mathit{\Gamma}_k^h}\left(\sum_{p=0}^{N_t}\frac{(2p+1)k^2}{|\Theta_p(k)|^2}\,j_p(k|z|)^2\right)^{-1}\right)^{1/2}, \tag{72}$$

where $\check{\Pi}$ is a regularized approximation of Π, and $\mathit{\Gamma}_k^h=c_{\text{o}}^{-1}\mathit{\Gamma}_\omega^h$. To facilitate the ensuing discussion, one may also introduce an auxiliary indicator function

$$\lambda_{N_t}(k)\;=\;\sum_{p=0}^{N_t}\frac{1}{j_p'(k)-\alpha_p(k)j_p(k)} \tag{73}$$

which, in light of (61), has the property that $\lambda_{N_t}(k)\to\infty$ as k approaches a transmission eigenvalue associated with $p_*\leqslant N_t$.

Examples. In what follows the featured obstacle configuration, $D=\{x\in\mathbb{R}^3:\,|x|<1\}$, is exercised numerically to highlight the existence of interior (Dirichlet or transmission) eigenvalues, and to assess their effect on the behavior of (71) and (72). As an illustration, the results are computed assuming frequency band $\mathit{\Gamma}_\omega=[10c_{\text{o}},15c_{\text{o}}]$ i.e. $\mathit{\Gamma}_k=[10,15]$ and truncation level $N_t=10$, chosen such that $|\sigma_p|<10^{-3}$, $p>N_t$ for all configurations examined, see (69). For completeness, obstacle reconstruction is effected assuming both "fine" discretization of $\mathit{\Gamma}_k$, namely

$$\mathit{\Gamma}_k^{h_1}:=\big\{k\colon k{=}10+m\,h_1,\ h_1{=}10^{-3},\ m{\in}\{0,1,\ldots,5\cdot10^3\}\big\}, \tag{74}$$

and four "coarse" discretizations

$$\begin{aligned} F_k^{h_2} &= \big\{10, 11, 12, 13, 14, 15\big\}, \\ F_k^{h_3} &= \big\{10, 11, 12, 13, 14.0662, 15\big\}, \\ F_k^{h_4} &= \big\{10, 11.25, 12.5, 13.75, 15\big\}, \\ F_k^{h_5} &= \big\{10, 11.25, 12.5664, 13.75, 15\big\}. \end{aligned}$$

Fig. 2(a) shows the variation of auxiliary indicator function (73) for a Dirichlet obstacle ($\beta \to \infty$), which clearly indicates the existence of Dirichlet eigenvalues within first N_t spherical harmonic modes of the truncated solution. The spatial distribution of $\check{\Pi}_F^{(1)}$ and $\check{\Pi}_F^{(2)}$ in the $z_3 = 0$ plane, as computed from (71) and (72) assuming $F_k^{h_1}$ as a discrete set of wavenumbers over which the far-field observations $u_\infty(\hat{x}, d)$, $\hat{x}, d \in \Omega$ are available,

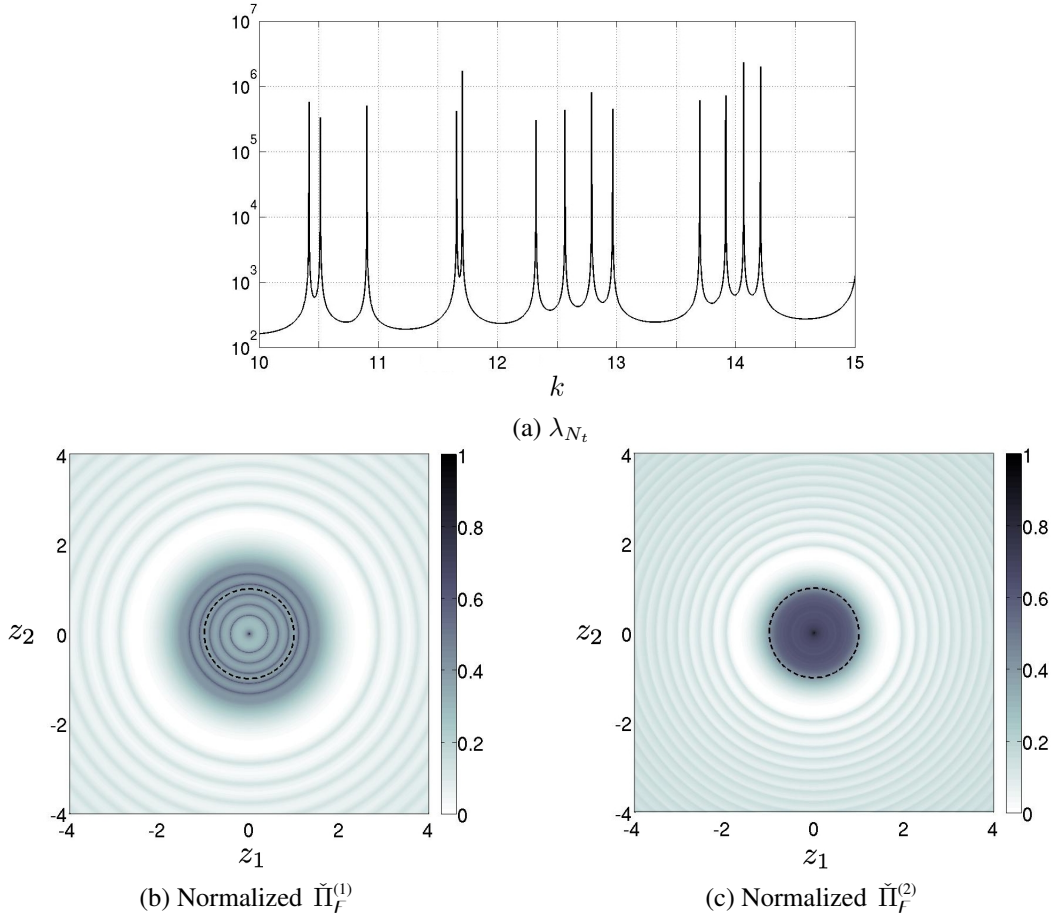

(a) λ_{N_t}

(b) Normalized $\check{\Pi}_F^{(1)}$

(c) Normalized $\check{\Pi}_F^{(2)}$

Figure 2: Reconstruction of a Dirichlet obstacle $(\beta \to \infty)$ from the far-field data taken over a "fine" wavenumber set $F_k^{h_1}$.

is plotted on a normalized scale $[0, 1]$ in Fig. 2(b) and 2(c). The featured indicator distributions, spherically symmetric due to assumed geometry of the problem, show that the "serial" indicator (71) is strongly affected by traversing the Dirichlet eigenvalues owing to its particular structure which requires that $\check{\Pi}_F^{(1)} \to 0$ uniformly in $\mathbb{R}^3$ as $\Theta_p(k) \to 0$, $p \in \{0, \ldots, N_t\}$. From (72) and Fig. 2(c), on the other hand, it is also apparent that the far-field observations u_∞ taken at "resonant" frequencies make only a *trivial* contribution to $\check{\Pi}_F^{(2)}$,

and thus do not degrade the quality of multi-frequency obstacle reconstruction when executed in terms of the latter indicator function. The above conclusions are further substantiated by the results in Fig. 3 which plots $\lambda_{N_t}(k)$, $\check{\Pi}_{\digamma}^{(1)}(z)$ and $\check{\Pi}_{\digamma}^{(2)}(z)$ for a sample penetrable-obstacle configuration, characterized by $\beta = 1$ and $\gamma = 2$. In particular, it is noted that the spatial distribution of $\check{\Pi}_{\digamma}^{(1)}$ plotted in Fig. 3(b) provides no visible clues as to the support of a hidden ball.

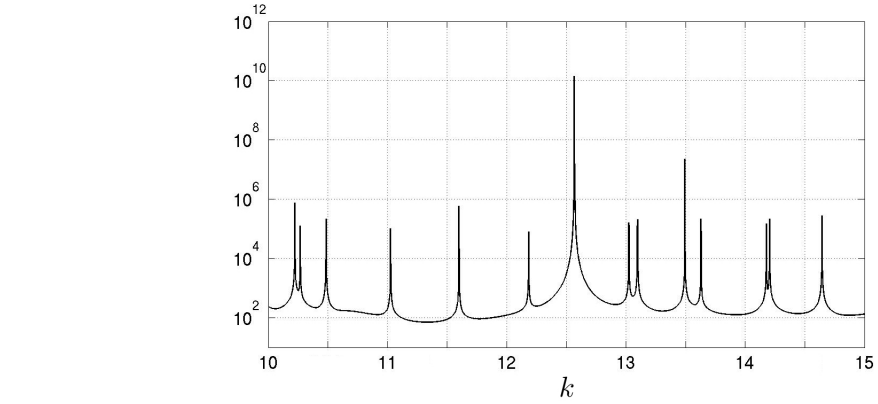

(a) λ_{N_t}

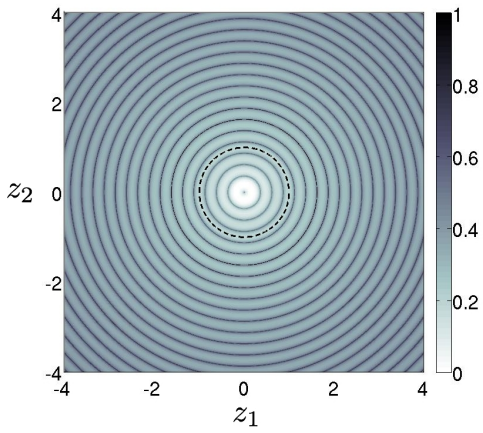

(b) Normalized $\check{\Pi}_{\digamma}^{(1)}$

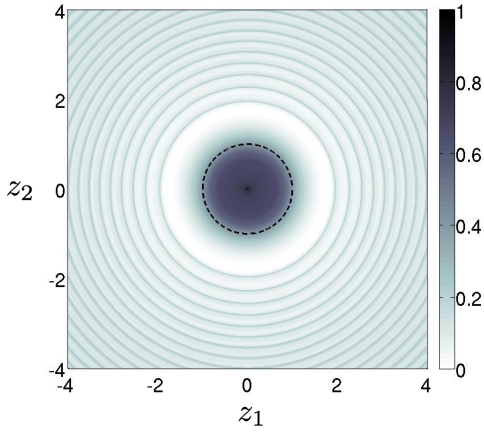

(c) Normalized $\check{\Pi}_{\digamma}^{(2)}$

Figure 3: Reconstruction of a penetrable obstacle $(\beta = 1, \gamma = 2)$ from the far-field data taken over a "fine" wavenumber set $\digamma_k^{h_1}$.

For completeness, the above Dirichlet and penetrable obstacle are each reconstructed anew using the far-field data from two "coarse" wavenumber sets. In particular, the Dirichlet obstacle is reconstructed in Figs. 4 and 5 from the data taken respectively over $\digamma_k^{h_2}$ and $\digamma_k^{h_3}$, designed such that $\digamma_{k^2}^{h_2} \cap \Lambda = \emptyset$ and $\digamma_{k^2}^{h_3} \cap \Lambda \neq \emptyset$, where Λ signifies the set of Dirichlet eigenvalues for a unit ball with sound speed $c_{\rm o}$. As can be seen from the display, both $\check{\Pi}_{\digamma}^{(1)}$ and $\check{\Pi}_{\digamma}^{(2)}$ (this time plotted versus $|z|$) appear to effectively reconstruct the obstacle on the basis of $\digamma_k^{h_2}$ while, commensurate with the earlier result, only $\check{\Pi}_{\digamma}^{(1)}$ succeeds when using $\digamma_k^{h_3}$ as the sampled set of wavenumbers. The same conclusion can be drawn from Figs. 6 and 7 which illustrate the reconstruction of a penetrable defect $(\beta = 1, \gamma = 2)$ on the basis of $\digamma_k^{h_4}$ and $\digamma_k^{h_5}$, chosen such that $\digamma_{k^2}^{h_4} \cap \Lambda = \emptyset$ and $\digamma_{k^2}^{h_5} \cap \Lambda \neq \emptyset$, where Λ denotes the germane (countable) set of transmission eigenvalues.

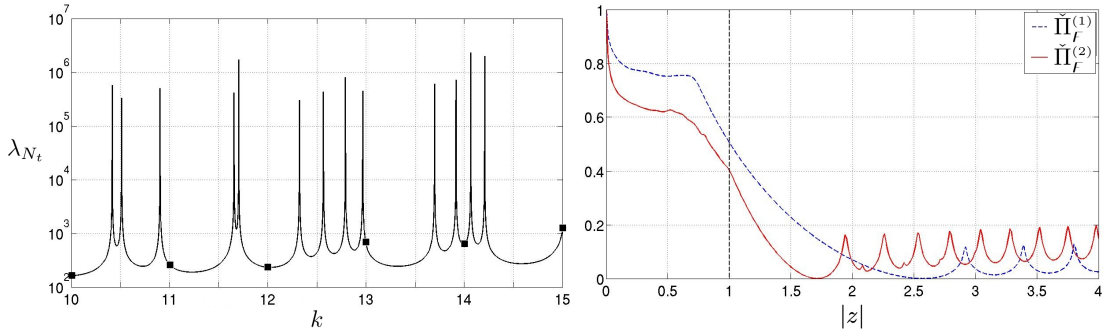

Figure 4: Reconstruction of a Dirichlet obstacle $(\beta \to \infty)$ from the far-field data taken over a "coarse" wavenumber set $F_k^{h_2}$ (indicated by markers), taken such that $\Lambda \cap F_{k^2}^{h_2} = \emptyset$.

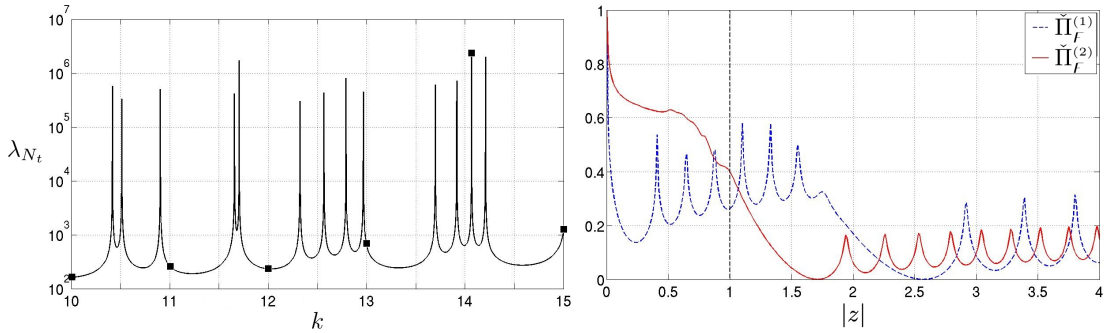

Figure 5: Reconstruction of a Dirichlet obstacle $(\beta \to \infty)$ from the far-field data taken over a "coarse" wavenumber set $F_k^{h_3}$ (indicated by markers), chosen such that $\Lambda \cap F_{k^2}^{h_3} \neq \emptyset$.

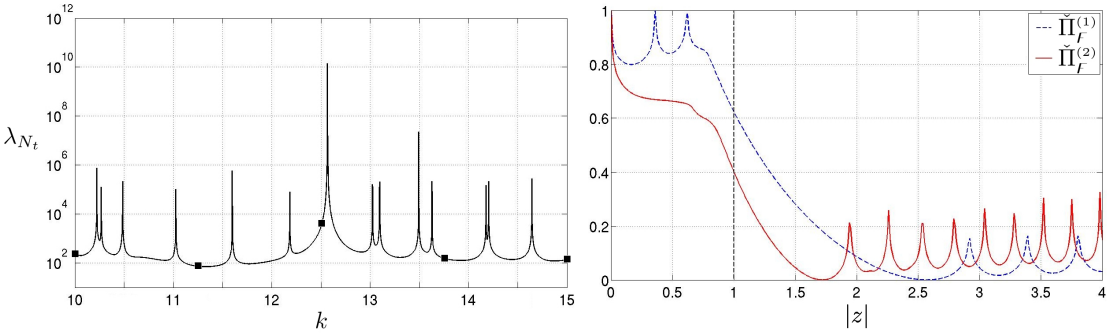

Figure 6: Reconstruction of a penetrable obstacle $(\beta = 1, \gamma = 2)$ from the far-field data taken over a "coarse" wavenumber set $F_k^{h_4}$ (indicated by markers), taken such that $\Lambda \cap F_{k^2}^{h_4} = \emptyset$.

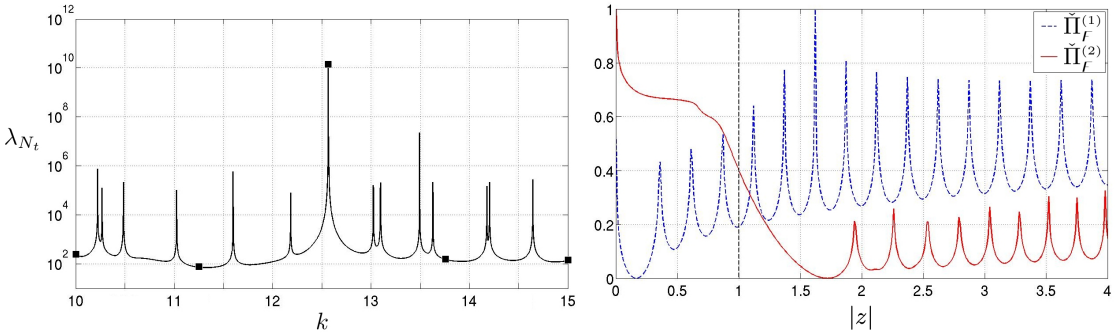

Figure 7: Reconstruction of a penetrable obstacle $(\beta = 1, \gamma = 2)$ from the far-field data taken over a "coarse" wavenumber set $F_k^{h_5}$ (indicated by markers), selected such that $\Lambda \cap F_{k^2}^{h_5} \neq \emptyset$.

5.2. Numerical study: square obstacle in $\mathbb{R}^2$

In this section the "multitonal" indicator functions (25) and (33) are applied to the inverse scattering of planes waves by a unit square, $D = \{x \in \mathbb{R}^2 : x \in [-0.5, 0.5] \times [-0.5, 0.5]\}$, assuming penetrable obstacle as in (51) with $n = 4$ and $\beta = 1/4$. To this end, a discrete set of directions of plane-wave incidence and observation is assumed as

$$\Omega^h := \big\{\hat{x} = \big(\cos(2\pi m h), \sin(2\pi m h)\big),\ h = \frac{1}{M},\ \ m \in \{0, 1, \ldots, M-1\}\big\}, \quad M = 61.$$

By analogy to (74), a "fine" discretization of the example wavenumber band $[3, 8]$ is taken as

$$\digamma_k^{h_6} := \big\{k\colon k = 3 + m\, h_6,\ h_6 = 5 \cdot 10^{-2},\ m \in \{0, 1, \ldots, 10^2\}\big\}.$$

Here it is noted that the featured interval $k^2 \in [9, 64] \subset \mathbb{R}$ contains, at least numerically, several transmission eigenvalues associated with the assumed scattering configuration in terms of D (see [**?**] for details).

For any fixed frequency $k \in \digamma_k^{h_6}$ and sampling point $z \in \mathbb{R}^2$, a discretized version of the *far-field* formulation (7) of the linear sampling method corresponding to $(\hat{x}, d) \in \Omega^h$ is written in the form

$$F_h\, g_{z,h} \ = \ f_{z,h}, \tag{75}$$

where F_h is a discretized far-field operator, and $f_{z,h} = (\Psi_\infty(\hat{x}, z, k))_{\hat{x} \in \Omega_h}$. To solve (75), the singular value decomposition of F_h is computed as $F_h = U\, S\, V^*$, where $U, V \in \mathbb{C}^{M \times M}$ are unitary matrices, V^* is the Hermitian transpose of V, and $S \in \mathbb{R}^{M \times M}$ a diagonal matrix such that $S_{jj} = \sigma_j$ is the jth singular value of F_h. With reference to (22), the norm of a Tikhonov-regularized solution $g_{z,h}^\epsilon$ to (75), with regularization parameter ϵ, is accordingly computed as

$$\|g_{z,h}^\epsilon\|^2_{L^2(\Omega_h)} \ = \ \sum_{j=1}^{M} \frac{\sigma_j^2}{(\sigma_j^2 + \epsilon)^2} |(U^* f_{z,h})_j|^2. \tag{76}$$

Fig. 8 plots the normalized distribution of indicator functions (25) and (33), on a scale $[0, 1]$, computed by way of (76) with $\epsilon = 10^{-4}$. Consistent with the earlier results, the two-dimensional reconstruction of a square scatterer via the "serial" indicator $\check{\Pi}_{\digamma}^{(1)}$ is inferior to that obtained using its "parallel" companion $\check{\Pi}_{\digamma}^{(2)}$, not only in terms of the contrast of an image, but also in terms of the reconstructed shape.

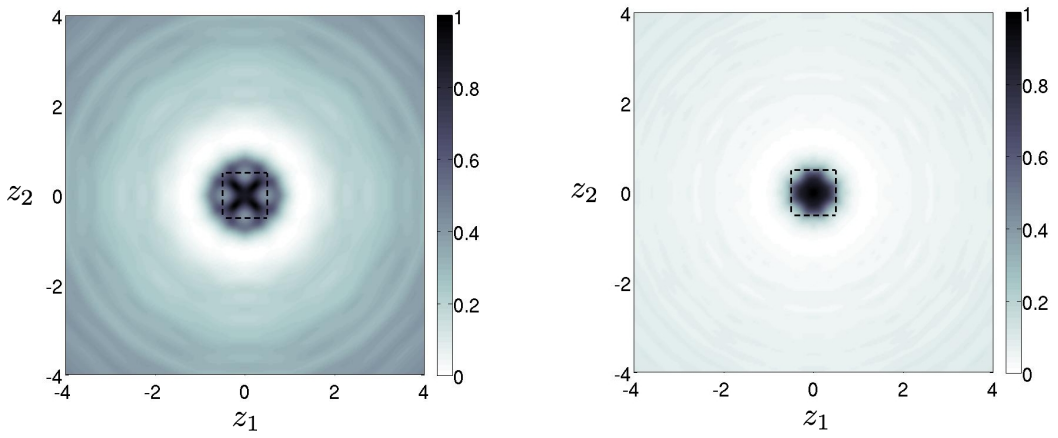

(a) Normalized $\check{\Pi}_f^{(1)}$ (b) Normalized $\check{\Pi}_f^{(2)}$

Figure 8: Reconstruction of a Dirichlet obstacle from the far-field data taken over a "fine" wavenumber set $\boldsymbol{F}_k^{h_6}$.

6. Conclusions

In this study, multi-frequency reconstruction of sound-soft and penetrable obstacles is examined in the context of the linear sampling method entailing either far-field or near-field measurements. On establishing a suitable approximate solution to the linear sampling equation under the premise of continuous frequency sweep, two possible choices for a cumulative multi-frequency indicator function of the scatterer's support are proposed. The first alternative, termed the "serial" indicator, is taken as a natural extension of its customary monochromatic counterpart in the sense that its computation entails *space-frequency* (as opposed to space) L^2-norm of a solution to the linear sampling equation. Under certain assumptions which include experimental observations down to zero frequency and compact frequency support of the wavelet used to illuminate the obstacle, this indicator function is further related to its time-domain companion. As a second possibility, the so-called "parallel" indicator is proposed as an L^2-norm, in the frequency domain, of the monochromatic indicator function. On the basis of the perturbation analysis which demonstrates that the monochromatic solution of the linear sampling equation behaves as $O(|k^2 - k_*^2|^{-m}),\ m \geqslant 1$ in the neighborhood of an isolated eigenvalue, k_*^2, of the associated interior (Dirichlet or transmission) problem, it is found that the "serial" indicator is unable to distinguish the interior from the exterior of a scatterer in situations when the prescribed frequency band traverses at least one such eigenvalue. In contrast the "parallel" indicator is, due to its particular structure, shown to be insensitive to the presence of pertinent interior eigenvalues (which typically form a countable set – unknown beforehand), and thus to be robust in a generic scattering environment. A set of numerical results, including both "fine" and "coarse" frequency sampling, is included to illustrate the performance of the competing (multi-frequency) indicator functions, demonstrating behavior that is consistent with the theoretical results.

Acknowledgment

The support provided by the University of Minnesota Supercomputing Institute, and by the U.S. Air Force Office of Scientific Research to F. Cakoni under Grant FA9550-08-1-0138, is kindly acknowledged. Special thanks are extended to Peter Monk for providing the linear sampling code and scattering data for the two-dimensional example, and to MTS Systems Corporation for providing the opportunity for F. Cakoni to visit the Department of Civil Engineering, University of Minnesota as an MTS Visiting Professor of Geomechanics.

References

[1] T. Arens. Why linear sampling works. *Inverse Problems*, 20:163–173, 2004.

[2] T. Arens and A Lechleiter. The linear sampling method revisited. *J. Integral Equations Appl.*, 21:179–202, 2009.

[3] C Bellis and B Guzina. A. *Journal of Elasticity*, pages 1–30, 2010.

[4] M. Bonnet. Inverse acoustic scattering by small-obstacle expansion of misfit function. *Inverse Problems*, page submitted, 2006.

[5] F. Cakoni and D. Colton. Combined far field operators in electromagnetic inverse scattering theory. *Math. Meth. Appl. Sci.*, 26:413–429, 2003.

[6] F. Cakoni and D. Colton. On the mathematical basis of the linear sampling method. *Georgian Math. J.*, 10:911–925, 2003.

[7] F. Cakoni and D. Colton. *Qualitative Methods in Inverse Scattering Theory*. Springer,-Verlag Berlin, 2006.

[8] F. Cakoni, D. Colton, and D. Gintides. The interior transmission eigenvalue problem. *under review*, pages 1–10, 2010.

[9] F. Cakoni, D. Colton, and H. Haddar. The linear sampling method for anisotropic media. *Journal of Computational and Applied Mathematics*, 146:285–299, 2002.

[10] F. Cakoni, D. Colton, and H. Haddar. On the determination of dirichlet and transmission eigenvalues from far field data. *C. R. Acad. Sci. Paris, Ser. I*, 348:379–383, 2010.

[11] F. Cakoni, D. Colton, and P. Monk. On the use of transmission eigenvalues to estimate the index of refraction from far field data. *Inverse Problems*, 23:507–522, 2007.

[12] F. Cakoni, D. Gintides, and H. Haddar. The existence of an infinite discrete set of transmission eigenvalues. *SIAM J. Math. Anal.*, 42:237–255, 2010.

[13] F. Cakoni and A. Kirsch. On the interior transmission eigenvalue problem. *Int. Jour. Comp. Sci. Math*, pages 1–24, 2010.

[14] Q. Chen, H. Haddar, A. Lechleiter, and P. Monk. A sampling method for inverse scattering in the time domain. *Inverse Problems*, 26:085001, 2010.

[15] F. Collino, M. Fares, and H. Haddar. A linear sampling method for the inverse transmission problem in near-field elastodynamics. *Inverse Problems*, 19:1279–1298, 2003.

[16] D. Colton, J. Coyle, and P. Monk. Recent developments in inverse acoustic scattering theory. *SIAM Review*, 42:369–414, 2000.

[17] D. Colton and A. Kirsch. A simple method for solving inverse scattering problems in the resonance region. *Inverse Problems*, 12:383–393, 1996.

[18] D. Colton and R. Kress. *Inverse acoustic and electromagnetic scattering theory*. Springer, Berlin, 1992.

[19] D. Colton, L. Paivarinta, and J. Sylvester. The interior transmission problem. *Inverse Problems and Imaging*, 1:13–28, 2006.

[20] D. Colton and B. D. Sleeman. An approximation property of importance in inverse scattering theory. *Proc. Edinburgh Math. Soc.*, 44:449–454, 2001.

[21] B. B. Guzina and M. Bonnet. Small-inclusion asymptotic for inverse problems in acoustics. *Inverse Problems*, 22:1761–85, 2006.

[22] B. B. Guzina and A. I. Madyarov. A linear sampling approach to inverse elastic scattering in piecewise-homogeneous domains. *Inverse Problems*, 23:1467–1493, 2007.

[23] T Kato. *Perturbation Theory for Linear Operators*. Springer, Berlin, Heidelberg, 1995.

[24] A. Kirsch. Characterization of the shape of a scattering obstacle using the spectral data of the far field operator. *Inverse Problems*, 14:1489–1512, 1998.

[25] A. Kirsch. The MUSIC-algorithm and the factorization method in inverse scattering theory for inhomogeneous media. *Inverse Problems*, 18:1025–1040, 2002.

[26] A. Kirsch. On the existence of transmission eigenvalues. *Inverse Problems and Imaging*, 3:155–172, 2009.

[27] A. Kirsch and N. Grinberg. *The Factorization Method for Inverse Problems*. Oxford University Press, New York, 2008.

[28] A. Kirsch and N. Grinberg. *The Factorization Method for Inverse Problems*. Oxford University Press, New York, 2008.

[29] C.D. Lines and S.N. Chandler-Wilde. A time domain point source method for inverse scattering by rough surfaces. *Computing*, 75:157–180, 2005.

[30] D.R. Luke. Multifrequency inverse obstacle scattering: the point source method and generalized filtered backprojection. *Math. Comput. Simul.*, 66:297–314, 2004.

[31] D.R. Luke and R. Potthast. The point source method for inverse scattering in the time domain. *MAth. Meth. Appl. Sci.*, 29:1501–1521, 2006.

[32] A. Malcolm and B. B. Guzina. On the topological sensitivity of transient acoustic fields. *Wave Motion*, 45:821–834, 2008.

[33] L. Paivarinta and J. Sylvester. Transmission eigenvalues. *SIAM Journal on Mathematical Analysis*, 40:738–753, 2008.

[34] I. G. Petrovskii. *Partial Differential Equations*. Iliffe Books LTD, London, 1967.

[35] F. Pockels. Uber die partielle differentialgleichung $\Delta u + k^2 u = 0$ and deren auftreten in die mathematischen physik. *Z. Math. Physik*, 37:100–105, 1892.

[36] B. Porat. *A Course in Digitial Signal Processing*. J. Wiley and Sons, 1996.

[37] R. Potthast. A fast new method to solve inverse scattering problems. *Inverse Problems*, 12:731–742, 1996.

[38] R. Potthast. A fast new method to solve inverse scattering problems. *IMA J. Appl. Math.*, 61:119–1140, 1998.

[39] R. Potthast. *Point Sources and Multipoles in Inverse Scattering Theory*. Chapman and Hal/ CRC, DNew York, 2001.

[40] B. P. Rynne and B. D. Sleeman. The interior transmission problem and inverse scattering from inhomogeneous media. *SIAM J. Math. Anal.*, 22:1755–1762, 1991.